

Published in final edited form as:

*Curr Neurovasc Res.* 2010 May ; 7(2): 95–112.

## Early Apoptotic Vascular Signaling is Determined by Sirt1 Through Nuclear Shuttling, Forkhead Trafficking, Bad, and Mitochondrial Caspase Activation

Jinling Hou<sup>1</sup>, Zhao Zhong Chong<sup>1</sup>, Yan Chen Shang<sup>1</sup>, and Kenneth Maiese<sup>1,2,3,4,5,\*</sup>

<sup>1</sup>Division of Cellular and Molecular Cerebral Ischemia, Wayne State University School of Medicine, Detroit, Michigan 48201, USA

<sup>2</sup>Departments of Neurology and Anatomy & Cell Biology, Wayne State University School of Medicine, Detroit, Michigan 48201, USA

<sup>3</sup>Barbara Ann Karmanos Cancer Institute, Wayne State University School of Medicine, Detroit, Michigan 48201, USA

<sup>4</sup>Translational Neuroscience Program, Wayne State University School of Medicine, Detroit, Michigan 48201, USA

<sup>5</sup>Institute of Environmental Health Sciences, Wayne State University School of Medicine, Detroit, Michigan 48201, USA

### Abstract

Complications of diabetes mellitus (DM) weigh heavily upon the endothelium that ultimately affect multiple organ systems. These concerns call for innovative treatment strategies that employ molecular pathways responsible for cell survival and longevity. Here we show in a clinically relevant model of DM with elevated D-glucose that endothelial cell (EC) SIRT1 is vital for the prevention of early membrane apoptotic phosphatidylserine externalization and subsequent DNA degradation supported by studies with modulation of SIRT1 activity and gene knockdown of *SIRT1*. Furthermore, during elevated D-glucose exposure, we show that SIRT1 is sequestered in the cytoplasm of ECs, but specific activation of SIRT1 shuttles the protein to the nucleus to allow for cytoprotection. The ability of SIRT1 to avert apoptosis employs the activation of protein kinase B (Akt1), the post-translational phosphorylation of the forkhead member FoxO3a, the blocked trafficking of FoxO3a to the nucleus, and the inhibition of FoxO3a to initiate a “pro-apoptotic” program as shown by complimentary gene knockdown studies of *FoxO3a*. Vascular apoptotic oversight by SIRT1 extends to the direct modulation of mitochondrial membrane permeability, cytochrome c release, Bad activation, and caspase 1 and 3 activation, since inhibition of SIRT1 activity and gene knockdown of *SIRT1* significantly accentuate cascade progression while SIRT1 activation abrogates these apoptotic elements. Our work identifies vascular SIRT1 and its control over early apoptotic membrane signaling, Akt1 activation, post-translational modification and trafficking of FoxO3a, mitochondrial permeability, Bad activation, and rapid caspase induction as new avenues for the treatment of vascular complications during DM.

## Keywords

Akt; Bad; caspase; cell demise; diabetes; endothelial; phosphatidylserine

---

## INTRODUCTION

Developed countries devote a significant portion of their gross domestic product to healthcare, but improved life expectancy for individuals of these nations usually poorly correlates with these expenditures [1]. These outcomes occur as a result of multiple factors, such as lifestyle, genetic, and environmental influences, that can affect disease progression. Diabetes mellitus (DM) is one disorder that exemplifies these influences and affects multiple systems of the body, not in the least are the hematological and vascular systems [2–8]. Both acute hyperglycemia as well as prolonged elevated levels of glucose can lead to oxidative stress [9] and result in early and late apoptotic injury programs in vascular endothelial cells (ECs) [10–12]. In addition, induction of early apoptotic membrane changes through the externalization of membrane phosphatidylserine (PS) residues can initiate phagocytosis by surrounding inflammatory cells and eventual degradation of nuclear DNA [13–15].

These observations point to the critical need for the elucidation of the molecular pathways that determine early apoptotic injury in the vascular system to lay the foundation for innovative treatment strategies for DM. One pathway that may fulfill this criteria involves the sirtuin (silent mating type information regulation 2 homolog) 1 (*S. cerevisiae*) (SIRT1), a NAD<sup>+</sup>-dependent deacetylase and the mammalian ortholog of the silent information regulator 2 (Sir2) protein that can control multiple processes such as cell survival, lifespan, and metabolism [16–19]. SIRT1 can deacetylate histones and multiple transcription factors [20–22]. Of these, the forkhead transcription factor FoxO3a and its upstream control by protein kinase B (Akt1) have high significance in the ability to oversee apoptotic injury and immune system modulation [23–28] and FoxO3a is of particular interest since polymorphisms of *FoxO3a* are associated with increased body mass [29] and risk for the development of DM.

Here we show that both vascular endogenous and exogenous SIRT1 control early and late programs of apoptosis in a clinically relevant model that examines one aspect of DM with elevated D-glucose that require the shuttling of SIRT1 to the cell nucleus to protect ECs. The presence of endogenous SIRT1 is vital for the prevention of early membrane apoptotic PS externalization and subsequent DNA degradation as demonstrated by our studies with manipulation of SIRT1 activity and gene knockdown of *SIRT1*. Furthermore, SIRT1 EC protection employs the activation of Akt1 and the post-translational phosphorylation and inhibition of FoxO3a that blocks trafficking of the “pro-apoptotic” FoxO3a from the cytoplasm to the EC nucleus. Gene knockdown studies of *FoxO3a* further support that loss of FoxO3a activity is a significant component for SIRT1 to block EC injury and apoptotic caspase activity during elevated D-glucose. Vascular apoptotic oversight by endogenous and exogenous SIRT1 extends to the modulation of mitochondrial membrane permeability, cytochrome c release, Bad activation, and pro-caspase 1 and 3 cleavage, since inhibition of SIRT1 activity and gene knockdown of *SIRT1* promote cascade initiation and progression while SIRT1 activation abrogates these apoptotic elements that are tied to the initiation of cellular membrane PS exposure and genomic DNA cleavage [30–34]. Our work is the first to highlight vascular SIRT1 and its intimate control over early apoptotic membrane signaling, Akt1 activation, post-translational modification and trafficking of FoxO3a, mitochondrial permeability, cytochrome c release, Bad phosphorylation, and rapid caspase induction as novel molecular therapeutic strategies for vascular degeneration and complications during DM.

## MATERIALS AND METHODS

### Cerebral Microvascular Endothelial Cell Cultures

All procedures were approved by the Institutional Animal Care and Use Committee of Wayne State University with protocol # A 09-05-09. All efforts were made to minimize the number of animals used and their suffering. Per our prior protocols, vascular endothelial cells (ECs) were isolated from male Sprague-Dawley adult rat brain cerebra by using a modified collagenase/dispase-based digestion protocol [35,36]. Briefly, ECs were cultured in endothelial growth media consisting of M199E (M199 with Eagle's salt) with 20% heat-inactivated fetal bovine serum, 2 mmol/l L-glutamine, 90 µg/ml heparin, and 20 µg/ml EC growth supplement (ICN Biomedicals, Aurora, OH). Cells from the third passage were identified by positive direct immunocytochemistry for factor VIII-related antigen [35,36] and possessed characteristic spindle-shaped morphology with antigenic properties shown to resemble brain endothelium *in vivo* [37]. All animal experimentation was conducted in accord with accepted standards of humane animal care and NIH guidelines.

### Experimental Treatments

Elevated D-glucose (or L-glucose as a control plus 5.6 mM D-glucose) concentrations in ECs was performed by replacing the media with serum-free M199E media with 2 mmol/l L-glutamine and 90 µg/ml heparin containing 20 mM D-glucose and then incubated at 37°C for 48 hours. For treatments applied prior to elevated D-glucose, application of sirtuin 1 (SIRT1) protein (Sigma-Aldrich, St Louis, MO), resveratrol (3,5,4'-trihydroxy-*trans*-stilbene) (Tocris Bioscience, Ellisville, MO), sirtinol (Sigma-Aldrich, St Louis, MO), or 6-chloro-2,3,4,9-tetrahydro-1*H*-carbazole-1-carboxamide (EX527, Tocris Bioscience, Ellisville, MO) were continuous.

### Assessment of Cell Survival

EC injury was determined by bright field microscopy using a 0.4% trypan blue dye exclusion method 48 hours following treatment with elevated D-glucose per our previous protocols [35,36]. The mean survival was determined by counting eight randomly selected non-overlapping fields with each containing approximately 10–20 cells (viable + non-viable). Each experiment was replicated 6 times independently with different cultures.

### Assessment of DNA Fragmentation

Genomic DNA fragmentation was determined by the terminal deoxynucleotidyl transferase nick end labeling (TUNEL) assay [38]. Briefly, ECs were fixed in 4% paraformaldehyde/0.2% picric acid/0.05% glutaraldehyde and the 3'-hydroxy ends of cut DNA were labeled with biotinylated dUTP using the enzyme terminal deoxytransferase (Promega, Madison, WI) followed by streptavidin-peroxidase and visualized with 3,3'-diaminobenzidine (Vector Laboratories, Burlingame, CA).

### Assessment of Membrane Phosphatidylserine (PS) Residue Externalization

Phosphatidylserine (PS) exposure was assessed through the established use of annexin V. A 30 µg/ml stock solution of annexin V conjugated to phycoerythrin (PE) (R&D Systems, Minneapolis, MN) was diluted to 3 µg/ml in warmed calcium containing binding buffer (10 mmol/L Hepes, pH 7.5, 150 mmol/L NaCl, 5 mmol/L KCl, 1 mmol/L MgCl<sub>2</sub>, 1.8 mmol/L CaCl<sub>2</sub>) [38]. Plates were incubated with 500 µl of diluted annexin V for 10 minutes. Images were acquired with "blinded" assessment with a Leitz DMIRB microscope (Leica, McHenry, IL) and a Fuji/Nikon Super CCD (6.1 megapixels) using transmitted light and fluorescent single excitation light at 490 nm and detected emission at 585 nm.

### Expression of SIRT1, Phosphorylated Akt1, Total Akt1, Phosphorylated FoxO3a, Total FoxO3a, Phosphorylated Bad, and Active Caspase 1 and 3

ECs were homogenized and each sample (50 µg/lane) was subjected to SDS-polyacrylamide gel electrophoresis (7.5% SIRT1, 7.5% Akt1, and FoxO3a; 12.5% Bad, caspase 1 and 3). After transfer, the membranes were incubated with a rabbit polyclonal antibody against SIRT1 (1: 200, Santa Cruz Biotechnologies, Santa Cruz, CA), a rabbit polyclonal antibody against phospho-Akt1 (Ser<sup>473</sup>, 1: 1000, Cell Signaling, Beverly, MA), a rabbit antibody against total Akt1, a rabbit polyclonal antibody against phospho-FoxO3a (1: 1000) (p-FoxO3a, Ser<sup>253</sup>, Cell Signaling, Beverly, MA), a rabbit antibody against total FoxO3a, a rabbit monoclonal antibody against phospho-Bad (Ser<sup>136</sup>, 1: 1000, Cell Signaling, Beverly, MA), and a rabbit antibody against cleaved (active) caspase 1 (20 kDa) (1: 1000), or a rabbit antibody against cleaved (active) caspase 3 (17 kDa) (1: 1000) (Cell signaling Technology, Beverly, MA). Following washing, the membranes were incubated with a horseradish peroxidase (HRP) conjugated secondary antibody goat anti-rabbit IgG (1: 2000, Zymed Laboratories, Carlsbad, CA). The antibody-reactive bands were revealed by chemiluminescence (Amersham Pharmacia Biotech, Piscataway, NJ) and band density was performed using the public domain NIH Image program (developed at the U.S. National Institutes of Health and available at <http://rsb.info.nih.gov/nih-image/>).

### SIRT1 Histone Deacetylase (HDAC) Activity Assay

ECs were homogenized and following protein determination, each sample (30 µg/10 µl) was used for SIRT1 activity measurement. SIRT1 histone deacetylase (HDAC) activity was determined with the use of SIRT1 Fluorimetric Drug Discovery Kit (Biomol International, Plymouth Meeting, PA) and following the manufacturer's protocol. EC protein extracts were incubated in assay buffer with β-nicotinamide adenine dinucleotide (NAD<sup>+</sup>) substrate at 37° C for 45 minutes. The fluorescence density was determined using a Multimode Detector (DTX880, Beckman Coulter, Brea, CA) and the relative activity of SIRT1 compared to untreated control ECs was used in the results.

### Gene Knockdown of *SIRT1* and *FoxO3a* with Small Interfering RNA (siRNA)

To silence *SIRT1* gene expression, the following sequences were synthesized (Applied Biosystems, Foster City, CA): the SIRT1 siRNA sense strand 5'-GCGAUGUUAUA AUUAAUGAtt-3' and the antisense strand 5'-UCAUUA AUUUAACAUCGCag-3'. To silence *FoxO3a* gene expression, the following sequences were synthesized (Applied Biosystems, Foster City, CA): the FoxO3a siRNA sense strand 5'-AUCUAACUCAUCUGCAAGUUU -3' and the antisense strand 5'-ACUUGCAGAUG AGUUAGAUUU -3'. Transfection of siRNA duplexes was performed with Lipofectamine 2000 reagent according to manufacturer guidelines (Invitrogen, Carlsbad, CA). Experimental assays were performed 72 hours post-transfection. For each siRNA assay, positive controls contain multiple siRNAs including the target siRNA and negative controls are absent of the target siRNA. In addition, following gene knockdown of *SIRT1* or *FoxO3a*, the expression of these proteins was assessed by immunofluorescence and western analysis. EC cultures were incubated with rabbit anti-SIRT1 (1: 100, Santa Cruz Biotechnologies, Santa Cruz, CA) or anti-FoxO3a (1: 100, Cell Signaling Technology, Beverly, MA) at 4° over night. After incubation with biotinylated anti-rabbit IgG (1: 50) (Vector Laboratories, Burlingame, CA) at room temperature for 2 hours, the expression was revealed by conjugation to fluorescein avidin (1: 50) (Vector Laboratories, Burlingame, CA).

### Assessment of Mitochondrial Membrane Potential

The fluorescent probe JC-1 (Molecular Probes, Eugene, OR), a cationic membrane potential indicator, was used to assess the mitochondrial membrane potential. ECs in 35 mm dishes were

incubated with 2 µg/ml JC-1 in growth medium at 37 °C for 30 min. The cultures were washed three times using fresh growth medium. Mitochondria were then analyzed immediately under a Leitz DMIRB microscope (Leica, McHenry, IL, USA) with a dual emission fluorescence filter with 515–545 nm for green fluorescence and emission at 585–615 nm for red fluorescence [38].

### **Preparation of Mitochondria for the Analysis of Cytochrome c Release**

After washing once with ice-cold PBS, cells were harvested at 10,000g for 15 min at 4°C and the resulting pellet was re-suspended in buffer A (20 mM HEPES, pH 7.5, 10 mM KCl, 1.5 mM MgCl<sub>2</sub>, 1 mM EDTA, 1 mM EGTA, 1 mM dithiothreitol, 0.1 phenylmethylsulfonylfluoride) containing 250 mM sucrose and used as the mitochondrial fraction. The supernatant was subjected to ultracentrifugation at 50,000 g for 1 hour at 4 °C with the resultant supernatant used as the cytosolic fraction [38].

### **Immunocytochemistry for SIRT1, FoxO3a, and Caspase 3**

For immunocytochemical staining of SIRT1, FoxO3a, or cleaved caspase 3 (active form), ECs were fixed with 4% paraformaldehyde and permeabilized using 0.2% Triton X-100. Cells were then incubated with rabbit anti-SIRT1 (1: 100, Santa Cruz Biotechnologies, Santa Cruz, CA), anti-FoxO3a (1: 100, Cell Signaling Technology, Beverly, MA) or rabbit anti-cleaved caspase 3 (1: 200, Cell Signaling Technology, Beverly, MA) over night at 4 °C and then with biotinylated anti-rabbit IgG (1: 50, Vector laboratories) for 2 hours followed by Texas Red streptavidin (1: 50, Vector laboratories) for 1 hour. Cells were washed in PBS, then stained with DAPI (Sigma, St. Louis, MO) for nuclear identification. SIRT1, FoxO3a, and caspase 3 proteins were imaged with fluorescence at the wavelengths of 565 nm (red) and 400 nm (DAPI nuclear staining).

### **Subcellular Translocation of SIRT1 or FoxO3a by Western Analysis**

ECs were initially homogenized. The cytoplasmic and nuclear proteins were subsequently prepared by using NEPER nuclear and cytoplasmic extraction reagents according to the instructions of the manufacturer (Pierce, Rockford, IL). The expression of SIRT1 or FoxO3a in the EC nucleus and cytoplasm was determined by Western analysis. Each sample (50 µg/lane) was subjected to 7.5% SDS-poly-acrylamide gel electrophoresis. After transfer, the membranes were incubated with a rabbit polyclonal antibody against SIRT1 (1: 200) (Santa Cruz Biotechnologies, Santa Cruz, CA) or a primary rabbit antibody against FoxO3a (1: 1000) (Cell Signaling, Beverly, MA). After washing, the membranes were incubated with a horseradish peroxidase conjugated with a secondary antibody (goat anti-rabbit IgG, 1: 2000) (Invitrogen, Carlsbad, CA). The antibody-reactive bands were revealed by chemiluminescence (Amersham Pharmacia Biotech, Piscataway, NJ) and band density was performed using the public domain NIH Image program (developed at the U.S. National Institutes of Health and available at <http://rsb.info.nih.gov/nih-image/>).

### **Statistical Analysis**

For each experiment, the mean and standard error were determined. Statistical differences between groups were assessed by means of analysis of variance (ANOVA) from 6 replicate experiments with the post-hoc Dunnett's test. Statistical significance was considered at  $P < 0.05$ .

## **RESULTS**

### **Progressive Concentrations of D-Glucose Lead to Reduced EC Survival**

Elevated D-glucose concentrations (10, 20, 50 and 75 mM) were administered to ECs and cell injury was assessed 48 hours later by the trypan blue dye exclusion method. In Fig. (1A),



representative images illustrate that elevated D-glucose treatment ( $\geq 20$  mM) leads to significant uptake of trypan blue in ECs consistent with cell membrane injury. Quantitative analysis shows EC survival is significantly diminished to  $53 \pm 5\%$  (20 mM),  $41 \pm 5\%$  (50 mM), and  $33 \pm 5\%$  (75 mM) after D-glucose administration when compared to untreated control cultures ( $98 \pm 3\%$ ,  $P < 0.01$ ) (Fig. 1B). Since a concentration of 20 mM D-glucose produced a survival rate of approximately 50% (a 50% EC injury loss), this concentration of elevated D-glucose was used for the remainder of the experimental studies.

In our ECs, we also demonstrate that hyperosmolarity or L-glucose do not play a significant role in EC toxicity (Fig. 1C). D-glucose (20 mM), L-glucose (20 mM), and mannitol (20 mM) were administered to ECs and cell injury with trypan blue (TB), apoptotic phosphatidylserine (PS) exposure, and apoptotic DNA fragmentation (TUNEL) were assessed 48 hours later. Elevated D-glucose (20 mM) resulted in significant labeling for TB, PS, and TUNEL when compared to untreated control cells, demonstrating that D-glucose results in EC injury with TB uptake and apoptosis with PS and TUNEL. In contrast, elevated L-glucose does not result in EC injury or apoptosis, illustrating that elevated D-glucose is specific for EC demise. Furthermore, a mannitol concentration of 20 mM had similar EC TB, PS, and TUNEL labeling to that of untreated control cells demonstrating that hyperosmolarity was not a significant factor in EC injury (Fig. 1C).

### **Elevated D-Glucose Exposure Diminishes Endogenous SIRT1 Expression and Blocks SIRT1 Shuttling to the Nucleus, but Nuclear Translocation is Preserved during SIRT1 Protein and agonist Administration**

Western blot assay was performed for the endogenous cellular expression of SIRT1 following elevated D-glucose (20 mM) administration. In Fig. (1D), expression of endogenous EC SIRT1 was significantly and progressively decreased at 6, 24, and 48 hours during elevated D-glucose (20 mM) exposure. This loss of SIRT1 expression correlates with progressive EC injury over a 48 hour period of elevated D-glucose administration.

We next examined the agents used in our study, activators of SIRT1 with SIRT1 protein (2  $\mu$ M) and resveratrol (15  $\mu$ M), and inhibitors of SIRT1 with EX527 (2  $\mu$ M) and sirtinol (75  $\mu$ M), to alter SIRT1 activity assessed by HDAC activity at 6 hours and 48 hours following elevated D-glucose (20 mM) exposure (Fig. 1E). Over a 48 hour course following elevated D-glucose, HDAC is decreased in ECs. In contrast, the SIRT1 activators SIRT1 protein (2  $\mu$ M) and resveratrol (15  $\mu$ M) significantly increase HDAC activity in ECs at 6 hours and 48 hours following elevated D-glucose exposure (Fig. 1E). Furthermore, the SIRT1 inhibitors EX527 (2  $\mu$ M) and sirtinol (75  $\mu$ M) markedly depress HDAC activity in ECs below untreated control EC levels at 6 hours and 48 hours following elevated D-glucose exposure (Fig. 1E).

Since loss of SIRT1 endogenous cellular expression may be detrimental to cells during toxin exposure [13,39] and nuclear translocation of SIRT1 may be required for cell survival and differentiation in other cell systems [40,41], we next examined the cellular trafficking of SIRT1 in ECs during elevated D-glucose administration (20 mM). We used immunofluorescent staining for SIRT1 and DAPI nuclear staining to follow the translocation of SIRT1 48 hours after elevated D-glucose exposure. Untreated control ECs in merged images do not have visible nuclei (red in color, white arrows) that illustrate nuclear localization of SIRT1. During elevated D-glucose exposure, a significant proportion of SIRT1 was confined to the cytoplasm of ECs as illustrated by minimal nuclear staining as shown with DAPI staining (blue nuclei in color) in the nucleus in ECs in merged images (Figs. 1F, 1G). In contrast, exogenous administration of SIRT1 protein (2  $\mu$ M) or administration of resveratrol (15  $\mu$ M) that is known to activate SIRT1 [42] in the presence of elevated D-glucose fostered the translocation of endogenous SIRT1 from the cytoplasm to the nucleus. This is evident by the inability to detect significant DAPI nuclear staining (blue in color) in cells during merged elevated images since SIRT1

staining is present in the nucleus of ECs (Figs. **1F, 1G**). Furthermore, application of the specific small-molecule inhibitor of SIRT1 catalytic activity EX527 (2  $\mu$ M) [43] during elevated D-glucose prevented the functional translocation of SIRT1 to the nucleus and maintained SIRT1 in the cytoplasm of ECs to a greater degree than during periods with only administration of elevated D-glucose alone (Figs. **1F, 1G**). We also assessed SIRT1 subcellular translocation from the cell cytoplasm to the nucleus through western analysis (Figs. **2A, 2B**). At 48 hours following elevated D-glucose (20 mM) (HG), SIRT1 remained confined to the cytoplasm of ECs. Yet, administration of SIRT1 protein (2  $\mu$ M) or resveratrol (15  $\mu$ M) promoted the translocation of endogenous SIRT1 from the cytoplasm to the nucleus during elevated D-glucose. In addition, inhibition of SIRT1 catalytic activity with EX527 (2  $\mu$ M) blocked the translocation of SIRT1 to the nucleus and maintained SIRT1 in the cytoplasm of ECs to a greater extent than during elevated D-glucose alone (Figs. **2A, 2B**).

### **SIRT1 Activation Protects against EC Injury during Elevated D-Glucose**

In Fig. (**2C**), representative figures show significant trypan blue staining in ECs 48 hours after elevated (high) D-glucose (20 mM) administration alone or during inhibition of SIRT1 activity with sirtinol (75  $\mu$ M) or EX527 (2  $\mu$ M) during elevated D-glucose (20 mM). In contrast, trypan blue uptake is significantly reduced in ECs during activation of SIRT1 with SIRT1 protein (2  $\mu$ M) or with resveratrol (15  $\mu$ M) in the presence of elevated D-glucose (20 mM). On further analysis in Figs. (**2D – G, EC**) survival was progressively increased during elevated D-glucose administration (20 mM) in the presence of increasing concentrations of the SIRT1 activators SIRT1 protein (0.5  $\mu$ M, 1  $\mu$ M, 2  $\mu$ M, and 5  $\mu$ M) or in the presence of resveratrol (5  $\mu$ M, 15  $\mu$ M, 30  $\mu$ M, and 100  $\mu$ M). Yet, application of increasing concentrations of the SIRT1 inhibitors sirtinol (25  $\mu$ M, 50  $\mu$ M, 75  $\mu$ M, and 100  $\mu$ M) or EX527 (0.5  $\mu$ M, 1  $\mu$ M, 2  $\mu$ M, and 5  $\mu$ M) led to progressive injury in ECs during elevated D-glucose administration (20 mM).

### **Gene Knockdown of *SIRT1* Leads to Increased EC Injury during Elevated D-Glucose Suggesting Endogenous Cellular Protection**

ECs were transfected with SIRT1 siRNA and the expression of SIRT1 protein was assessed by immunocytochemistry and Western blot analysis 6 hours following elevated D-glucose (20 mM) administration (Figs. **3A – 3C**). Gene knockdown of *SIRT1* in either untreated control ECs or in ECs exposed to elevated D-glucose alone resulted in absent expression of SIRT1 protein (Figs. **3A – 3C**). As a control, non-specific scrambled SIRT1 siRNA did not alter SIRT1 protein expression in untreated control cells or cells exposed to elevated D-glucose, illustrating the specificity of SIRT1 siRNA to block protein expression of SIRT1 (Figs. **3B** and **3C**). In Fig. (**3D**), representative figures illustrate significant trypan blue staining in ECs 48 hours after elevated D-glucose (20 mM) administration alone or with elevated D-glucose during scrambled (non-specific) siRNA. In addition, more pronounced trypan blue uptake is present in ECs following elevated D-glucose with SIRT1 siRNA transfection (Fig. **3D**), demonstrating that loss of endogenous SIRT1 not only leads to EC injury, but also prevents a minimal level of EC protection during elevated D-glucose administration that is present in ECs not transfected with SIRT1 siRNA. Quantitation of results in Fig. (**3E**) show that EC survival was significantly decreased from  $56 \pm 5\%$  during elevated D-glucose administration alone to  $25 \pm 5\%$  ( $P < 0.01$ ) during transfection with SIRT1 siRNA 48 hours after elevated D-glucose administration. Transfection with scrambled siRNA did not alter EC injury during elevated D-glucose exposure.

### **SIRT1 Activation Blocks Apoptotic Early Phosphatidylserine (PS) Exposure and Later Nuclear DNA Degradation during Elevated D-Glucose**

In representative Figs. (**4A** and **4C**), untreated control ECs were without DNA fragmentation assessed by TUNEL or PS externalization assessed by annexin V. In ECs exposed to elevated

D-glucose (20 mM), significant DNA fragmentation (TUNEL) and membrane PS exposure (annexin V) occurs 48 hours after exposure. In Figs. (4A – 4D), elevated D-glucose (20 mM) led to a significant increase in percent DNA fragmentation and membrane PS exposure in ECs 48 hours after elevated D-glucose compared to untreated control cultures for DNA ( $5 \pm 2\%$ ) and for PS ( $2 \pm 1\%$ ) respectively. Furthermore, during inhibition of SIRT1 activity with EX527 (2  $\mu$ M) or during gene knockdown of *SIRT1* with siRNA, EC DNA fragmentation and membrane PS exposure was worsened in the presence of elevated D-glucose (20 mM), suggesting that an endogenous level of SIRT1 provides some protection against apoptotic early and late programs (Figs. 4A – 4D). Transfection with non-specific scrambled siRNA did not alter DNA fragmentation or PS exposure in ECs in untreated controls or during elevated D-glucose. During activation of SIRT1 with SIRT1 protein (2  $\mu$ M) or with resveratrol (15  $\mu$ M) in the presence of elevated D-glucose (20 mM) EC DNA fragmentation and membrane PS exposure was significantly prevented, demonstrating that SIRT1 blocks apoptotic programs during elevated glucose (Figs. 4A – 4D).

### **SIRT1 leads to Akt1 Activation and Maintains the Inhibitory Phosphorylation of p-FoxO3a and Relies Upon p-FoxO3a Inhibition for EC Protection**

As a novel transcription factor closely tied to cell survival, activation of FoxO3a can initiate “pro-apoptotic” programs [36,44]. In addition, Akt1 is a principal mediator of the inhibitory phosphorylation of FoxO3a that can block activity of this transcription factor [45]. Absence of phosphorylated (active) Akt1 leads to the loss of post-translational phosphorylation of FoxO3a and prevents association of FoxO3a with 14-3-3 proteins to allow FoxO3a to translocate to the cell nucleus and initiate a “pro-apoptotic” program [36,44]. Since unphosphorylated FoxO3a can translocate to the cell nucleus [46,47], we investigated the ability of SIRT1 to control phosphorylation of both Akt1 and FoxO3a at 6, 24, and 48 hours following elevated D-glucose (20 mM) administration. Western blot assay was performed for phosphorylated Akt1 (p-Akt1), total Akt1, and FoxO3a (p-FoxO3a) at the preferential phosphorylation site for Akt1 of Ser<sup>253</sup> as well as for the expression of total FoxO3a (Figs. 5A – 5F). At 6 hours following elevated D-glucose (20 mM) administration, Akt1 phosphorylation and activity was increased, but was subsequently lost and returned to control levels or below at 24 hours and 48 hours after elevated D-glucose (Figs. 5A and 5B). Activation of SIRT1 with SIRT1 protein (2  $\mu$ M) or with resveratrol (15  $\mu$ M) in the presence of elevated D-glucose (20 mM) maintained the activity and phosphorylation of Akt1 during 6 hours, 24 hours, and 48 hours. In addition, expression of total Akt1 did not change illustrating that only the phosphorylation status of Akt1 was altered by SIRT1 activation.

Expression of phosphorylated (inactive) p-FoxO3a was initially increased at 6 hours and subsequently significantly decreased at 24 and 48 hours following elevated D-glucose (20 mM) administration. This activity and phosphorylation of FoxO3a directly corresponded to Akt1 activity with loss of Akt1 phosphorylation during elevated D-glucose resulting in the expression of active (unphosphorylated) FoxO3a at 24 and 48 hours (Figs. 5A – 5D). In addition, activation of SIRT1 with SIRT1 protein (2  $\mu$ M) or with resveratrol (15  $\mu$ M) maintained the expression of phosphorylated FoxO3a at 6, 24, and 48 hours to a greater degree than during elevated D-glucose (20 mM) exposure alone. However, inhibition of SIRT1 activity with EX527 (2  $\mu$ M) led to the loss of p-FoxO3a expression below levels for elevated D-glucose alone at 6 hours, 24 hours, and 48 hours (Figs. 5C, 5D). In Figs. (5E and 5F), gene knockdown of *SIRT1* with siRNA in ECs significantly reduced p-FoxO3a expression at 6 hours below levels observed with elevated D-glucose alone, but expression of total FoxO3a remained unchanged, demonstrating that the loss of SIRT1 protein only affected phosphorylation of FoxO3a and that the total FoxO3a protein was not degraded. In addition to the ability of SIRT1 to maintain expression of inactive p-FoxO3a during elevated D-glucose exposure, SIRT1 also requires the inactivation of FoxO3a to offer cellular protection in ECs during elevated D-



glucose. In Fig. (5G), gene knockdown of *FoxO3a* (see Figs. (8E and 8F) for knockdown efficiency) increased EC survival during elevated D-glucose alone and also produced equal protective capacity in ECs assessed by trypan blue uptake during either SIRT1 protein (2  $\mu$ M) or resveratrol (15  $\mu$ M) application at 48 hours after elevated D-glucose (20 mM), illustrating that SIRT1 activation relies upon the inhibition of FoxO3a activity. In addition, transfection of ECs with FoxO3a siRNA was able to reverse the detrimental effects of EC injury during elevated D-glucose alone and during SIRT1 inhibition with EX527 (2  $\mu$ M) (Fig. 5G). Transfection with scrambled FoxO3a siRNA did not prevent EC injury during elevated D-glucose alone or during EX527 administration (data not shown). Taken together, these results suggest that SIRT1 is dependent upon the prevention of FoxO3a activity to exert protection in ECs.

### **SIRT1 Controls Subcellular Trafficking of FoxO3a and Maintains FoxO3a in the Cytoplasm of ECs during Elevated Glucose**

Post-translational phosphorylation of FoxO3a results in the association with 14-3-3 proteins to sequester FoxO3a in the cytoplasm and block the nuclear transcription of “pro-apoptotic” proteins [36,44]. Given the ability of SIRT1 to maintain post-translational phosphorylation of FoxO3a, we next examined whether SIRT1 controls subcellular trafficking of FoxO3a. In ECs, we performed immunofluorescent staining for FoxO3a and DAPI nuclear staining to follow the subcellular translocation of FoxO3a 48 hours after elevated D-glucose administration (20 mM) (Figs. 6A, 6B). In the presence of elevated D-glucose, immunofluorescent staining for FoxO3a in the nucleus of ECs is markedly present. This is evident by the inability to visualize DAPI nuclear staining (blue in color) in cells during merged elevated images since prominent FoxO3a staining is present in the nucleus (Fig. 6A). In addition, either inhibition of SIRT1 activity with EX527 (2  $\mu$ M) or transfection with SIRT1 siRNA during elevated D-glucose exposure also allows the translocation of FoxO3a from the cell cytoplasm to the nucleus in ECs (Figs. 6A, 6B). Interestingly, gene knockdown of *SIRT1* yields significantly greater nuclear translocation of FoxO3a than elevated D-glucose exposure alone or during application of non-specific scrambled siRNA in the presence of elevated D-glucose, illustrating the specificity for SIRT1 siRNA as well as the ability of endogenous SIRT1 to influence the subcellular trafficking of FoxO3a (Figs. 6A, 6B). Furthermore, activation of SIRT1 with SIRT1 protein (2  $\mu$ M) or resveratrol (15  $\mu$ M) administration maintained FoxO3a in the cytoplasm of ECs similar to untreated control cells demonstrating minimal nuclear staining as shown with DAPI staining (blue nuclei in color) in the nucleus merged images (Figs. 6A, 6B). We complemented the immunofluorescent studies with assessment of FoxO3a subcellular translocation from the cell cytoplasm to the nucleus through western analysis (Figs. 6C, 6D). Consistent with our immunofluorescent work, activation of SIRT1 with SIRT1 protein (2  $\mu$ M) or resveratrol (15  $\mu$ M) maintains FoxO3a in the cytoplasm of ECs similar to untreated control ECs, but inhibition of SIRT1 activity with EX527 (2  $\mu$ M) during elevated D-glucose allows the translocation of FoxO3a from the cell cytoplasm to the nucleus in ECs (Figs. 6C, 6D).

### **SIRT1 Blocks Mitochondrial Depolarization, Cytochrome c Release, and Activation of Bad**

Mitochondrial depolarization in ECs was assessed during elevated D-glucose by the cationic membrane potential indicator JC-1. In Figs. (7A and 7B), elevated D-glucose (20 mM) yielded a significant decrease in the EC mitochondrial red/green fluorescence intensity ratio within 24 hours ( $43 \pm 3\%$ ) when compared to untreated control mitochondria ( $100 \pm 6\%$ ), demonstrating that elevated D-glucose results in mitochondrial membrane depolarization. Inhibition of SIRT1 activity with EX527 (2  $\mu$ M) (Fig. 7A and 7B) or gene knockdown of *SIRT1* with siRNA (Figs. 7A and 7B) during elevated D-glucose resulted in a more pronounced depolarization of the mitochondria with a ratio of  $19 \pm 2\%$  and  $18 \pm 2\%$  respectively. Non-specific scrambled siRNA produced similar mitochondrial depolarization during elevated D-glucose when compared to elevated D-glucose alone (Figs. 7A and 7B). However, activation of SIRT1 with SIRT1 protein

(2  $\mu$ M) or with resveratrol (15  $\mu$ M) in the presence of elevated D-glucose significantly increased the red/green fluorescence intensity of the mitochondria to  $77 \pm 4\%$  and  $75 \pm 3\%$  respectively, illustrating that activation of SIRT1 can significantly improve mitochondrial permeability transition pore membrane potential (Figs. **7A** and **7B**).

Elevated D-glucose (20 mM) within 24 hours also produced a significant release of cytochrome c from the mitochondria to a  $3.0 \pm 0.2$  fold increase when compared to untreated control mitochondria using western analysis (Figs. **7C** and **7D**). Inhibition of SIRT1 activity with EX527 (2  $\mu$ M) (Figs. **7C** and **7D**) or transfection with SIRT1 siRNA (Figs. **7E** and **7F**) during elevated D-glucose were unable to block the release of cytochrome c and also result in a more prominent release of cytochrome c when compared to D-glucose exposure alone. Non-specific scrambled siRNA did not alter this release of cytochrome c during elevated D-glucose exposure (Figs. **7E** and **7F**). Yet, the activation of SIRT1 with administration of SIRT1 protein (2  $\mu$ M) or resveratrol (15  $\mu$ M) during elevated D-glucose actively prevented cytochrome c release to a similar degree that occurs with untreated control EC mitochondria (Figs. **7C** and **7D**).

Since SIRT1 relies upon Akt1 to control FoxO3a, we hypothesized that SIRT1 also may govern Bad that is localized in the outer mitochondrial membrane and when phosphorylated by Akt1 can bind to protein 14-3-3 to release Bcl-x<sub>L</sub> and prevent apoptosis [48–52]. Western blot assay was performed for phosphorylated Bad (p-Bad) at the preferential phosphorylation site for Akt1 of Ser<sup>136</sup> (Figs. **7G**, **7H**). At 24 hours following elevated D-glucose (20 mM) administration, Bad phosphorylation and activity was significantly reduced. Activation of SIRT1 with SIRT1 protein (2  $\mu$ M) or with resveratrol (15  $\mu$ M) in the presence of elevated D-glucose (20 mM) significantly increased the phosphorylation and activity of Bad at 24 hours. Furthermore, loss of SIRT1 during gene knockdown decreased the activity of Bad to a greater degree than during exposure to elevated D-glucose alone (Figs. **7G**, **7H**).

### **SIRT1 Attenuates Caspase 1 and Caspase 3 Activation during Elevated D-Glucose Exposure that Relies Upon FoxO3a**

Given that SIRT1 controls mitochondrial membrane permeability, we next investigated whether SIRT1 also affects caspase 3 and caspase 1 activity since mitochondrial release of cytochrome c results in apoptotic caspase activation [53–55]. Within 24 hours following elevated D-glucose (20 mM) exposure, immunocytochemistry reveals significant cleaved (active) caspase 3 (blue/red staining) during elevated D-glucose alone, during the inhibition of SIRT1 activity with EX527 (2  $\mu$ M), or during gene knockdown of *SIRT1* with siRNA. Inhibition of SIRT1 activity with EX527 and loss of SIRT1 with siRNA transfection also significantly increased caspase 3 activity, but non-specific scrambled siRNA combined with elevated D-glucose administration did not alter caspase 3 activity when compared to exposure to elevated D-glucose alone, illustrating that endogenous SIRT1 offers protection against caspase 3 activation in ECs. Furthermore, activation of SIRT1 with SIRT1 protein (2  $\mu$ M) or with resveratrol (15  $\mu$ M) in the presence of elevated D-glucose in ECs significantly blocks caspase 3 activity as evidenced by primarily blue immunocytochemical staining and by reducing the percentage of cleaved caspase 3 labeling to  $21 \pm 3\%$  and  $26 \pm 3\%$  respectively from  $50 \pm 3\%$  in ECs exposed to elevated D-glucose alone (Figs. **8A** and **8B**).

In Figs. (**8C**, **8D**, **8G** and **8H**), the expression of cleaved (active) caspase 3 and caspase 1 on western analysis were assessed at 24 hours following elevated D-glucose (20 mM) exposure and demonstrates significant caspase 3 and caspase 1 activities. Transfection with SIRT1 siRNA or inhibition of SIRT1 activity with EX527 (2  $\mu$ M) notably did not block caspase activity, but did result in a significant elevation in caspase 3 and caspase 1 activities supporting the premise that endogenous SIRT1 in ECs offers underlying protection against the apoptotic activation of caspase 3 and caspase 1 (Figs. **8C**, **8D**, **8G** and **8H**). Non-specific scrambled siRNA did not accelerate an increase in caspase 3 and caspase 1 activities during elevated D-

glucose exposure, further supporting the specific ability of SIRT1 to control caspase 3 and caspase 1 activities. In addition, SIRT1 activation with SIRT1 protein (2  $\mu$ M) or with resveratrol (15  $\mu$ M) markedly prevented the expression of cleaved caspase 3 and caspase 1 during elevated D-glucose (Figs. **8C**, **8D**, **8G** and **8H**).

We next evaluated the ability of FoxO3a to control caspase activity at the 24 hour period following elevated D-glucose (20 mM) administration in ECs. In Figs. (**8E** and **8F**), gene knockdown of *FoxO3a* in ECs exposed to elevated D-glucose (20 mM) resulted in absent expression of FoxO3a protein (Figs. **8E** and **8F**). As a control, non-specific scrambled FoxO3 siRNA did not alter FoxO3a protein expression in cells exposed to elevated D-glucose, demonstrating the specificity of FoxO3a siRNA to block protein expression of FoxO3a (Figs. **8E** and **8F**). Expression of cleaved active caspase 3 and caspase 1 (Figs. **8G** and **8H**) is elevated almost 4 fold over untreated control EC levels following elevated D-glucose, but transfection with FoxO3a siRNA significantly blocks cleaved active caspase 3 and caspase 1 activities. Non-specific scrambled siRNA was not effective in reducing caspase 3 or caspase 1 activity during elevated D-glucose, further supporting the specific role for FoxO3a to control caspase 3 and caspase 1 activity during elevated D-glucose in ECs (Figs. **8G** and **8H**).

## DISCUSSION

Employing an elevated D-glucose model for primary ECs, we show that progressively elevated concentrations of D-glucose lead to a significant loss in EC survival and result in apoptotic membrane PS externalization and nuclear DNA fragmentation. A final D-glucose concentration of 20 mM injures approximately 60% of ECs and leads to significant apoptosis, illustrating that primary cerebral ECs are extremely sensitive to elevations in D-glucose to a greater degree than vascular cells from other sources such as human umbilical vein ECs that require elevated D-glucose concentrations at > 25 mM for 3–5 days exposure to generate apoptotic injury [56]. Furthermore, the elevated D-glucose concentrations used in our study are similar to clinical glucose concentrations not only during poorly controlled diabetes [57–59], but also during early onset diabetes [60] and during expected diurnal variations with diabetes [9,61] known to occur in a range from 15 mM–25 mM (270 mg/dl–450 mg/dl). In addition, hyperosmolarity did not play a significant role in EC injury, since a mannitol concentration of 20 mM resulted in similar and not significantly different survival rates than untreated control ECs. We performed additional studies with the biologically inactive agent L-glucose and also observed that L-glucose in concentrations of 20 mM did not significantly alter EC survival.

SIRT1 has been associated with the loss of insulin sensitivity [62] and a poor response to fasting plasma glucose levels in adipocytes [63]. Activation of SIRT1 also can prevent endothelial senescence during hyperglycemia [64] and reduce endothelial atherosclerotic lesions during elevated lipid states [65], suggesting an important role for SIRT1 in DM. In addition, elevated glucose in endothelial progenitor cells decreases SIRT1 expression when examined three days later and leads to diminished endothelial progenitor cell numbers [66]. We demonstrate that endogenous SIRT1 expression in cerebral ECs is more rapidly affected by elevated D-glucose and progressively lost at 6, 24, and 48 hours after elevated D-glucose exposure. Our studies also show that progressive activation of SIRT1 with increasing concentrations of SIRT1 protein or resveratrol protects ECs against elevated D-glucose. However, loss of SIRT1 activity, such as during inhibition with sirtinol or EX527, or during gene knockdown of *SIRT1*, results in significant EC injury and is worse than treatment with elevated D-glucose alone, illustrating that endogenous SIRT1 also affords a level of protection in ECs during elevated D-glucose exposure.

Although primarily a nuclear protein [20,50], SIRT1 can shuttle between the cell nucleus and cytoplasm, such as in cardiomyocytes and neural precursor cells. SIRT1 cell trafficking to the cell nucleus may be necessary for cell survival and differentiation [40,41]. Using both western analysis and immunocytochemistry, our work shows that nuclear localization of SIRT1 may be vital for EC protection. During activation of SIRT1 which is cytoprotective against elevated D-glucose, we demonstrate that SIRT1 is maintained in the nucleus of ECs. However, during non-cytoprotective regimens such as during elevated D-glucose alone or during blockade of SIRT1 catalytic activity with elevated D-glucose, SIRT1 remains confined to the cytoplasm of ECs.

In regards to apoptotic cell injury [15,31,55], externalization of membrane PS residues during apoptosis can promote hypercoagulable states [67,68] and alert inflammatory cells to eliminate ECs tagged with PS [30,32,38,69]. SIRT1 has been associated with reduced apoptotic nuclear DNA degradation in islet beta cells [70] and with the prevention of membrane PS externalization in neurons [13,39] and in lymphoblastoid cell lines [71]. In our model of ECs during elevated D-glucose exposure, we have specifically identified the ability of SIRT1 to prevent early apoptotic membrane PS externalization and subsequent nuclear DNA degradation. Pharmacological activation of SIRT1 blocks the early and late programs of apoptosis, but inhibition of SIRT1 or gene knockdown of *SIRT1* does not prevent EC apoptotic program induction.

The ability of SIRT1 to limit EC apoptotic injury during elevated D-glucose requires the activation of Akt1, the post-translational phosphorylation of FoxO3a, and the maintenance of FoxO3a in the cytoplasm of ECs. In other models of oxidative stress or DM [49,72,73], activation of SIRT1 results in cellular protection and has been associated with enhanced activity of Akt. Akt1 is known to phosphorylate FoxO3a [74] and block the activity of this transcription factor [45], but loss of Akt1 activity allows FoxO3a to translocate to the cell nucleus and initiate apoptosis [36,44]. We now show that the inhibitory phosphorylation of FoxO3a directly corresponds to Akt1 activity that is mediated by the activation of SIRT1. In essence, SIRT1 results in the activation of Akt1 that is able to phosphorylate and inhibit FoxO3a over a 48 hour period during elevated D-glucose exposure. In addition, absence of SIRT1 activity through pharmacological inhibition or gene knockdown results in the loss of Akt1 activity and the loss of inhibitory FoxO3a phosphorylation without changes to total FoxO3a expression, illustrating that total FoxO3a is present and not degraded and that SIRT1 is required to specifically target and inhibit FoxO3a through Akt1.

SIRT1 also is directly dependent upon the removal of FoxO3a activity and the maintenance of FoxO3a in the cytoplasm to prevent EC injury during elevated D-glucose. We show that gene knockdown of *FoxO3a* not only increases EC survival during elevated D-glucose alone, but also yields increased survival in ECs to a similar degree during SIRT1 activation illustrating that SIRT1 activation relies upon the inhibition of FoxO3a activity. In addition, transfection of ECs with FoxO3a siRNA also rescues ECs during inhibition of SIRT1 activity with EX527, further supporting that loss of FoxO3a activity is a significant component for SIRT1 to block EC injury during elevated D-glucose. We also demonstrate with both western analysis and immunofluorescent studies that activation of SIRT1 with the subsequent phosphorylation of FoxO3a prevents the subcellular trafficking of FoxO3a from the cytoplasm to the EC nucleus and maintains FoxO3a in the cytoplasm to prevent the onset of apoptosis by FoxO3a during elevated D-glucose exposure. Prior work has shown that unphosphorylated (active) FoxO3a is able to disassociate from 14-3-3 proteins in the cytosol of cells and subsequently translocate to the cell nucleus to initiate “pro-apoptotic” transcriptional activity [36,44].

Mitochondrial membrane permeability plays a significant role in the determination of cell survival and the initiation of the apoptotic cascade [75–77], especially during periods of

elevated glucose and DM [11,78–80]. Agents that activate sirtuins can reduce the release of mitochondrial reactive oxygen species during elevated glucose [81]. We show that elevated D-glucose in ECs leads to mitochondrial membrane depolarization and the release of cytochrome c. However, SIRT1 activation maintains physiological mitochondrial membrane function and prevents the release of cytochrome c during elevated D-glucose. In contrast, inhibition of SIRT1 activity or gene knockdown of *SIRT1* results in the pronounced loss of mitochondrial membrane permeability and the release of cytochrome c.

Since SIRT1 relies upon the activation of Akt1, we also examined the activity of the mitochondrial associated protein Bad, a pro-apoptotic Bcl-2 family member that becomes active by Akt1 through the phosphorylation on its serine residues. Unphosphorylated Bad is localized on the outer mitochondrial membrane and binds to the anti-apoptotic Bcl-2 family member Bcl-x<sub>L</sub> through its BH3 domain. Subsequent phosphorylation of Bad by Akt1 leads to the binding of Bad with the cytosolic protein 14-3-3 to release Bcl-x<sub>L</sub> and prevent apoptosis [48–52]. We now show that SIRT1 also significantly activates and increases the phosphorylation of Bad during elevated D-glucose. Furthermore, loss of SIRT1 during gene knockdown decreases the activity of Bad to a greater degree than during exposure to elevated D-glucose alone, demonstrating that endogenous SIRT1 is a significant component in ECs for the control of mitochondrial permeability, cytochrome c release, and the activity of Bad during elevated D-glucose.

Pharmacological activation of SIRT1 in injury paradigms with chondrocytes [82] and retinal cells [83] can reduce caspase activity. We therefore examined the ability of SIRT1 to control apoptotic caspase 3 and caspase 1 activities in ECs during elevated D-glucose. We demonstrate that elevated D-glucose initiates a significant activation of caspase 3 and caspase 1, but that SIRT1 activation significantly attenuates caspase 3 and 1 activities during elevated D-glucose exposure. Yet, blockade of SIRT1 activity or gene knockdown of *SIRT1* enhances the activities of these proteases, illustrating that endogenous SIRT1 also provides protection against apoptotic caspase activation in ECs during elevated D-glucose exposure. Furthermore, we show that the control of FoxO3a by SIRT1 is a necessary component for the prevention of caspase 3 and caspase 1 activities. Prior studies have demonstrated that caspase 3 may bind to FoxO3a [84–86] and that FoxO3a has been associated with increases in caspase 3 and caspase 6 activities in melanoma cells and inflammatory cells [27,28,87]. We show that expression of the active (unphosphorylated) form of FoxO3a at 24 hours following elevated D-glucose directly correlates with robust caspase 3 and 1 activities at this time. In addition, gene knockdown of *FoxO3a* abrogates the activities of caspase 3 and caspase 1, illustrating the significant role FoxO3a plays in caspase 3 and caspase 1 activity.

Complications in the endothelial vascular system during DM requires innovative development of novel treatment strategies responsible for cell survival and longevity [50,68,88–91]. Our present studies demonstrate that through a series of intimately linked pathways for cell survival, SIRT1 governs early PS membrane and late DNA fragmentation apoptotic injury programs, activity of Akt1, phosphorylation and cell trafficking of FoxO3a, mitochondrial membrane permeability, cytochrome c release, Bad activity, and caspase 3 and caspase 1 activities. Our work highlights novel considerations for SIRT1 and its tightly integrated cellular pathways as new avenues for the early prevention and treatment of vascular disorders and related complications during DM.

## Acknowledgments

This research was supported by the following grants to Kenneth Maiese: American Diabetes Association, American Heart Association (National), Bugher Foundation Award, Janssen Neuroscience Award, LEARN Foundation Award, MI Life Sciences Challenge Award, Nelson Foundation Award, NIH NIEHS (P30 ES06639), NIH NIA, NIH NINDS, and NIH ARRA.



## REFERENCES

1. Development OfEC-0a. OECD Health Data 2009. 2009. Available at: [www.cosante.org/oeed.htm](http://www.cosante.org/oeed.htm)
2. Gossai D, Lau-Cam CA. The effects of taurine, taurine homologs and hypotaurine on cell and membrane antioxidative system alterations caused by type 2 diabetes in rat erythrocytes. *Adv Exp Med Biol* 2009;643:359–368. [PubMed: 19239167]
3. Guarnieri G, Zanetti M, Vinci P, Cattin MR, Barazzoni R. Insulin resistance in chronic uremia. *J Ren Nutr* 2009;19(1):20–24. [PubMed: 19121765]
4. Huber JD, VanGilder RL, Houser KA. Streptozotocin-induced diabetes progressively increases blood-brain barrier permeability in specific brain regions in rats. *Am J Physiol Heart Circ Physiol* 2006;291(6):H2660–H2668. [PubMed: 16951046]
5. Liu W, Liu P, Tao S, et al. Berberine inhibits aldose reductase and oxidative stress in rat mesangial cells cultured under high glucose. *Arch Biochem Biophys* 2008;475(2):128–134. [PubMed: 18471986]
6. Maiese K. Triple play: promoting neurovascular longevity with nicotinamide, WNT, and erythropoietin in diabetes mellitus. *Biomed Pharmacother* 2008;62(4):218–232. [PubMed: 18342481]
7. Maiese K, Morhan SD, Chong ZZ. Oxidative stress biology and cell injury during type 1 and type 2 diabetes mellitus. *Curr Neurovasc Res* 2007;4(1):63–71. [PubMed: 17311546]
8. Singh DK, Winocour P, Farrington K. Erythropoietic stress and anemia in diabetes mellitus. *Nat Rev Endocrinol* 2009;5(4):204–210. [PubMed: 19352318]
9. Monnier L, Mas E, Ginet C, et al. Activation of oxidative stress by acute glucose fluctuations compared with sustained chronic hyperglycemia in patients with type 2 diabetes. *JAMA* 2006;295(14):1681–1687. [PubMed: 16609090]
10. Ceriello A, dello Russo P, Amstad P, Cerutti P. High glucose induces antioxidant enzymes in human endothelial cells in culture. Evidence linking hyperglycemia and oxidative stress. *Diabetes* 1996;45(4):471–477. [PubMed: 8603769]
11. Chong ZZ, Shang YC, Maiese K. Vascular injury during elevated glucose can be mitigated by erythropoietin and Wnt signaling. *Curr Neurovasc Res* 2007;4(3):194–204. [PubMed: 17691973]
12. Yano M, Hasegawa G, Ishii M, et al. Short-term exposure of high glucose concentration induces generation of reactive oxygen species in endothelial cells: implication for the oxidative stress associated with postprandial hyperglycemia. *Redox Rep* 2004;9(2):111–116. [PubMed: 15231066]
13. Chong ZZ, Maiese K. Enhanced tolerance against early and late apoptotic oxidative stress in mammalian neurons through nicotinamidase and sirtuin mediated pathways. *Curr Neurovasc Res* 2008;5(3):159–170. [PubMed: 18691073]
14. Kang JQ, Chong ZZ, Maiese K. Akt1 protects against inflammatory microglial activation through maintenance of membrane asymmetry and modulation of cysteine protease activity. *J Neurosci Res* 2003;74(1):37–51. [PubMed: 13130504]
15. Soares MM, King SW, Thorpe PE. Targeting inside-out phosphatidylserine as a therapeutic strategy for viral diseases. *Nat Med* 2008;14(12):1357–1362. [PubMed: 19029986]
16. Canto C, Auwerx J. Caloric restriction, SIRT1 and longevity. *Trends Endocrinol Metab* 2009;20(7):325–331. [PubMed: 19713122]
17. Maiese K. Diabetic stress: new triumphs and challenges to maintain vascular longevity. *Expert Rev Cardiovasc Ther* 2008;6(3):281–284. [PubMed: 18327989]
18. Taylor DM, Maxwell MM, Luthi-Carter R, Kazantsev AG. Biological and potential therapeutic roles of sirtuin deacetylases. *Cell Mol Life Sci* 2008;65(24):4000–4018. [PubMed: 18820996]
19. Zschoernig B, Mahlknecht U. SIRTUIN 1: regulating the regulator. *Biochem Biophys Res Commun* 2008;376(2):251–255. [PubMed: 18774777]
20. Li F, Chong ZZ, Maiese K. Cell Life Versus Cell Longevity: The Mysteries Surrounding the NAD (+) Precursor Nicotinamide. *Curr Med Chem* 2006;13(8):883–895. [PubMed: 16611073]
21. Porcu M, Chiarugi A. The emerging therapeutic potential of sirtuin-interacting drugs: from cell death to lifespan extension. *Trends Pharmacol Sci* 2005;26(2):94–103. [PubMed: 15681027]
22. Saunders LR, Verdin E. Sirtuins: critical regulators at the crossroads between cancer and aging. *Oncogene* 2007;26(37):5489–5504. [PubMed: 17694089]

23. Chong ZZ, Li F, Maiese K. Activating Akt and the brain's resources to drive cellular survival and prevent inflammatory injury. *Histol Histopathol* 2005;20(1):299–315. [PubMed: 15578447]
24. Jonsson H, Allen P, Peng SL. Inflammatory arthritis requires Foxo3a to prevent Fas ligand-induced neutrophil apoptosis. *Nat Med* 2005;11(6):666–671. [PubMed: 15895074]
25. Maiese K, Chong ZZ, Shang YC. OutFOXOing disease and disability: the therapeutic potential of targeting FoxO proteins. *Trends Mol Med* 2008;14(5):219–227. [PubMed: 18403263]
26. Ogg S, Paradis S, Gottlieb S, et al. The Fork head transcription factor DAF-16 transduces insulin-like metabolic and longevity signals in *C. elegans*. *Nature* 1997;389(6654):994–999. [PubMed: 9353126]
27. Shang YC, Chong ZZ, Hou J, Maiese K. The forkhead transcription factor FoxO3a controls microglial inflammatory activation and eventual apoptotic injury through caspase 3. *Curr Neurovasc Res* 2009;6(1):20–31. [PubMed: 19355923]
28. Shang YC, Chong ZZ, Hou J, Maiese K. FoxO3a governs early microglial proliferation and employs mitochondrial depolarization with caspase 3, 8, and 9 cleavage during oxidant induced apoptosis. *Curr Neurovasc Res* 2009;6(4):223–238. [PubMed: 19807657]
29. Kim JR, Jung HS, Bae SW, et al. Polymorphisms in FOXO gene family and association analysis with BMI. *Obesity (Silver Spring, Md)* 2006;14(2):188–193.
30. Jessel R, Haertel S, Socaciu C, Tykhonova S, Diehl HA. Kinetics of apoptotic markers in exogenously induced apoptosis of EL4 cells. *J Cell Mol Med* 2002;6(1):82–92. [PubMed: 12003671]
31. Maiese K, Li F, Chong ZZ. New avenues of exploration for erythropoietin. *JAMA* 2005;293(1):90–95. [PubMed: 15632341]
32. Mallat M, Marin-Teva JL, Cheret C. Phagocytosis in the developing CNS: more than clearing the corpses. *Curr Opin Neurobiol* 2005;15(1):101–107. [PubMed: 15721751]
33. Mari C, Karabiyikoglu M, Goris ML, et al. Detection of focal hypoxic-ischemic injury and neuronal stress in a rodent model of unilateral MCA occlusion/reperfusion using radiolabeled annexin V. *Eur J Nucl Med Mol Imaging* 2004;31(5):733–739. [PubMed: 14985868]
34. Takahashi H, Nakamura S, Asano K, et al. Fas antigen modulates ultraviolet B-induced apoptosis of SVHK cells: sequential activation of caspases 8, 3, and 1 in the apoptotic process. *Exp Cell Res* 1999;249(2):291–298. [PubMed: 10366428]
35. Chong ZZ, Kang JQ, Maiese K. Erythropoietin is a novel vascular protectant through activation of Akt1 and mitochondrial modulation of cysteine proteases. *Circulation* 2002;106(23):2973–2979. 3. [PubMed: 12460881]
36. Chong ZZ, Maiese K. Erythropoietin involves the phosphatidylinositol 3-kinase pathway, 14-3-3 protein and FOXO3a nuclear trafficking to preserve endothelial cell integrity. *Br J Pharmacol* 2007;150(7):839–850. [PubMed: 17339844]
37. Abbott NJ, Hughes CC, Revest PA, Greenwood J. Development and characterisation of a rat brain capillary endothelial culture: towards an *in vitro* blood-brain barrier. *J Cell Sci* 1992;103(Pt 1):23–37. [PubMed: 1429907]
38. Kang JQ, Chong ZZ, Maiese K. Critical role for Akt1 in the modulation of apoptotic phosphatidylserine exposure and microglial activation. *Mol Pharmacol* 2003;64(3):557–569. [PubMed: 12920191]
39. Balan V, Miller GS, Kaplun L, et al. Life span extension and neuronal cell protection by Drosophila nicotinamidase. *J Biol Chem* 2008;283(41):27810–27819. [PubMed: 18678867]
40. Hisahara S, Chiba S, Matsumoto H, et al. Histone deacetylase SIRT1 modulates neuronal differentiation by its nuclear translocation. *Proc Natl Acad Sci USA* 2008;105(40):15599–15604. [PubMed: 18829436]
41. Tanno M, Sakamoto J, Miura T, Shimamoto K, Horio Y. Nucleocytoplasmic shuttling of the NAD<sup>+</sup>-dependent histone deacetylase SIRT1. *J Biol Chem* 2007;282(9):6823–6832. [PubMed: 17197703]
42. Tang BL, Chua CE. SIRT1 and neuronal diseases. *Mol Aspects Med* 2008;29(3):187–200. [PubMed: 17397914]
43. Solomon JM, Pasupuleti R, Xu L, et al. Inhibition of SIRT1 catalytic activity increases p53 acetylation but does not alter cell survival following DNA damage. *Mol Cell Biol* 2006;26(1):28–38. [PubMed: 16354677]

44. Zhu W, Bijur GN, Styles NA, Li X. Regulation of FOXO3a by brain-derived neurotrophic factor in differentiated human SH-SY5Y neuroblastoma cells. *Brain Res Mol Brain Res* 2004;126(1):45–56. [PubMed: 15207915]
45. Maiese K, Chong ZZ, Hou J, Shang YC. New strategies for Alzheimer's disease and cognitive impairment. *Oxid Med Cell Longev* 2009;2(5):279–290.
46. Hou J, Chong ZZ, Shang YC, Maiese K. FoxO3a governs early and late apoptotic endothelial programs during elevated glucose through mitochondrial and caspase signaling. *Mol Cell Endocrinol* 2010;321:194–206. [PubMed: 20211690]
47. Maiese K, Shang YC, Chong ZZ, Hou J. Diabetes mellitus: channeling care through cellular discovery. *Curr Neurovasc Res* 2010;7(1):59–64. [PubMed: 20158461]
48. Chong ZZ, Li F, Maiese K. Oxidative stress in the brain: Novel cellular targets that govern survival during neurodegenerative disease. *Prog Neurobiol* 2005;75(3):207–246. [PubMed: 15882775]
49. Chong ZZ, Lin SH, Li F, Maiese K. The sirtuin inhibitor nicotinamide enhances neuronal cell survival during acute anoxic injury through Akt, Bad, PARP, and mitochondrial associated 'anti-apoptotic' pathways. *Curr Neurovasc Res* 2005;2(4):271–285. [PubMed: 16181120]
50. Maiese K, Chong ZZ, Hou J, Shang YC. The vitamin nicotinamide: translating nutrition into clinical care. *Molecules* 2009;14(9):3446–3485. [PubMed: 19783937]
51. Morissette M, Al Sweidi S, Callier S, Di Paolo T. Estrogen and SERM neuroprotection in animal models of Parkinson's disease. *Mol Cell Endocrinol* 2008;290(1–2):60–69. [PubMed: 18515001]
52. Schlecht-Bauer D, Antier D, Machet MC, Hyvelin JM. Short- and long-term cardioprotective effect of darbepoetin-alpha: role of bcl-2 family proteins. *J Cardiovasc Pharmacol*. 2009 [Epub ahead of print].
53. Hao J, Shen W, Tian C, et al. Mitochondrial nutrients improve immune dysfunction in the type 2 diabetic Goto-Kakizaki rats. *J Cell Mol Med* 2009;13(4):701–711. [PubMed: 18410524]
54. Leuner K, Hauptmann S, Abdel-Kader R, et al. Mitochondrial dysfunction: the first domino in brain aging and Alzheimer's disease? *Antioxid Redox Signal* 2007;9(10):1659–1675. [PubMed: 17867931]
55. Maiese K, Chong ZZ, Li F, Shang YC. Erythropoietin: Elucidating new cellular targets that broaden therapeutic strategies. *Prog Neurobiol* 2008;85:194–213. [PubMed: 18396368]
56. Li Y, Wu H, Khardori R, et al. Insulin-like growth factor-1 receptor activation prevents high glucose-induced mitochondrial dysfunction, cytochrome-c release and apoptosis. *Biochem Biophys Res Commun* 2009;384(2):259–264. [PubMed: 19406106]
57. Maiese K, Chong ZZ, Hou J, Shang YC. Oxidative stress: Biomarkers and novel therapeutic pathways. *Exp Gerontol* 2010;45:217–234. [PubMed: 20064603]
58. Maiese K, Chong ZZ, Shang YC, Hou J. A "FOXO" in sight: targeting Foxo proteins from conception to cancer. *Med Res Rev* 2009;29(3):395–418. [PubMed: 18985696]
59. Pagano G, Bargero G, Vuolo A, Bruno G. Prevalence and clinical features of known type 2 diabetes in the elderly: a population-based study. *Diabet Med* 1994;11(5):475–479. [PubMed: 8088126]
60. Ryan EA, Imes S, Wallace C. Short-term intensive insulin therapy in newly diagnosed type 2 diabetes. *Diabetes Care* 2004;27(5):1028–1032. [PubMed: 15111515]
61. Troisi RJ, Cowie CC, Harris MI. Diurnal variation in fasting plasma glucose: implications for diagnosis of diabetes in patients examined in the afternoon. *JAMA* 2000;284(24):3157–3159. [PubMed: 11135780]
62. Weyrich P, Machicao F, Reinhardt J, et al. SIRT1 genetic variants associate with the metabolic response of Caucasians to a controlled lifestyle intervention--the TULIP Study. *BMC Med Genet* 2008;9:100. [PubMed: 19014491]
63. Yoshizaki T, Milne JC, Imamura T, et al. SIRT1 exerts anti-inflammatory effects and improves insulin sensitivity in adipocytes. *Mol Cell Biol* 2009;29(5):1363–1374. [PubMed: 19103747]
64. Orimo M, Minamino T, Miyauchi H, et al. Protective role of SIRT1 in diabetic vascular dysfunction. *Arterioscler Thromb Vasc Biol* 2009;29(6):889–894. [PubMed: 19286634]
65. Zhang QJ, Wang Z, Chen HZ, et al. Endothelium-specific overexpression of class III deacetylase SIRT1 decreases atherosclerosis in apolipoprotein E-deficient mice. *Cardiovasc Res* 2008;80(2):191–199. [PubMed: 18689793]

66. Balestrieri ML, Rienzo M, Felice F, et al. High glucose downregulates endothelial progenitor cell number *via* SIRT1. *Biochim Biophys Acta* 2008;1784(6):936–945. [PubMed: 18423418]
67. Dombroski D, Balasubramanian K, Schroit AJ. Phosphatidylserine expression on cell surfaces promotes antibody- dependent aggregation and thrombosis in beta2-glycoprotein I-immune mice. *J Autoimmun* 2000;14(3):221–229. [PubMed: 10756084]
68. Maiese K, Chong ZZ, Shang YC. Ravas and risks for erythropoietin. *Cytokine Growth Factor Rev* 2008;19(2):145–155. [PubMed: 18299246]
69. Chong ZZ, Kang J, Li F, Maiese K. mGluRI targets microglial activation and selectively prevents neuronal cell engulfment through akt and caspase dependent pathways. *Curr Neurovasc Res* 2005;2(3):197–211. [PubMed: 16181114]
70. Deng X, Cheng J, Zhang Y, Li N, Chen L. Effects of caloric restriction on SIRT1 expression and apoptosis of islet beta cells in type 2 diabetic rats. *Acta Diabetol.* 2009 [Epub ahead of print].
71. Olaharski AJ, Rine J, Marshall BL, et al. The flavoring agent dihydrocoumarin reverses epigenetic silencing and inhibits sirtuin deacetylases. *PLoS Genet* 2005;1(6):e77. [PubMed: 16362078]
72. Hasegawa K, Wakino S, Yoshioka K, et al. Sirt1 protects against oxidative stress-induced renal tubular cell apoptosis by the bidirectional regulation of catalase expression. *Biochem Biophys Res Commun* 2008;372(1):51–56. 18. [PubMed: 18485895]
73. Ni YG, Wang N, Cao DJ, et al. FoxO transcription factors activate Akt and attenuate insulin signaling in heart by inhibiting protein phosphatases. *Proc Natl Acad Sci USA* 2007;104(51):20517–20522. [PubMed: 18077353]
74. Maiese K, Hou J, Chong ZZ, Shang YC. A fork in the path: developing therapeutic inroads with FoxO proteins. *Oxid Med Cell Longev* 2009;2(3):119–126.
75. Astiz M, de Alaniz MJ, Marra CA. Effect of pesticides on cell survival in liver and brain rat tissues. *Ecotoxicol Environ Saf* 2009;72(7):2025–2032. [PubMed: 19493570]
76. Campos-Esparza MR, Sanchez-Gomez MV, Matute C. Molecular mechanisms of neuroprotection by two natural antioxidant polyphenols. *Cell Calcium* 2009;45(4):358–368. [PubMed: 19201465]
77. Chong ZZ, Kang JQ, Maiese K. Akt1 drives endothelial cell membrane asymmetry and microglial activation through Bcl-x(L) and caspase 1, 3, and 9. *Exp Cell Res* 2004;296(2):196–207. [PubMed: 15149850]
78. El-Mir MY, Detaille D, R-Villanueva G, et al. Neuroprotective role of antidiabetic drug metformin against apoptotic cell death in primary cortical neurons. *J Mol Neurosci* 2008;34(1):77–87. [PubMed: 18040888]
79. Newsholme P, Haber EP, Hirabara SM, et al. Diabetes associated cell stress and dysfunction: role of mitochondrial and non-mitochondrial ROS production and activity. *J Physiol* 2007;583(Pt 1):9–24. [PubMed: 17584843]
80. Plecita-Hlavata L, Lessard M, Santorova J, Bewersdorf J, Jezek P. Mitochondrial oxidative phosphorylation and energetic status are reflected by morphology of mitochondrial network in INS-1E and HEP-G2 cells viewed by 4Pi microscopy. *Biochim Biophys Acta* 2008;1777(7–8):834–846. [PubMed: 18452700]
81. Ungvari Z, Labinsky N, Mukhopadhyay P, et al. Resveratrol attenuates mitochondrial oxidative stress in coronary arterial endothelial cells. *Am J Physiol Heart Circ Physiol* 2009;297(5):H1876–H1881. [PubMed: 19749157]
82. Takayama K, Ishida K, Matsushita T, et al. SIRT1 regulation of apoptosis of human chondrocytes. *Arthritis Rheum* 2009;60(9):2731–2740. [PubMed: 19714620]
83. Anekonda TS, Adamus G. Resveratrol prevents antibody-induced apoptotic death of retinal cells through upregulation of Sirt1 and Ku70. *BMC Res Notes* 2008;1:122. [PubMed: 19046449]
84. Charvet C, Alberti I, Luciano F, et al. Proteolytic regulation of Forkhead transcription factor FOXO3a by caspase-3-like proteases. *Oncogene* 2003;22(29):4557–4568. [PubMed: 12881712]
85. Chong ZZ, Li F, Maiese K. Group I metabotropic receptor neuroprotection requires akt and its substrates that govern FOXO3a, bim, and beta-catenin during oxidative stress. *Curr Neurovasc Res* 2006;3(2):107–117. [PubMed: 16719794]
86. Chong ZZ, Lin SH, Maiese K. The NAD<sup>+</sup> precursor nicotinamide governs neuronal survival during oxidative stress through protein kinase B coupled to FOXO3a and mitochondrial membrane potential. *J Cereb Blood Flow Metab* 2004;24(7):728–743. [PubMed: 15241181]

87. Gomez-Gutierrez JG, Souza V, Hao HY, et al. Adenovirus-mediated gene transfer of FKHL1 triple mutant efficiently induces apoptosis in melanoma cells. *Cancer Biol Ther* 2006;5(7):875–883. [PubMed: 16861905]
88. Aso Y, Suganuma R, Wakabayashi S, et al. Anemia is associated with an elevated serum level of high-molecular-weight adiponectin in patients with type 2 diabetes independently of renal dysfunction. *Transl Res* 2009;154(4):175–182. [PubMed: 19766961]
89. Maiese K, Hou J, Chong ZZ, Shang YC. Erythropoietin, forkhead proteins, and oxidative injury: biomarkers and biology. *Sci World J* 2009;9:1072–1104.
90. McIntyre RS, Rasgon NL, Kemp DE, et al. Metabolic syndrome and major depressive disorder: co-occurrence and pathophysiologic overlap. *Curr Diab Rep* 2009;9(1):51–59. [PubMed: 19192425]
91. Rebecchi KR, Wenke JL, Go EP, Desaire H. Label-free quantitation: a new glycoproteomics approach. *J Am Soc Mass Spectrom* 2009;20(6):1048–1059. [PubMed: 19278867]



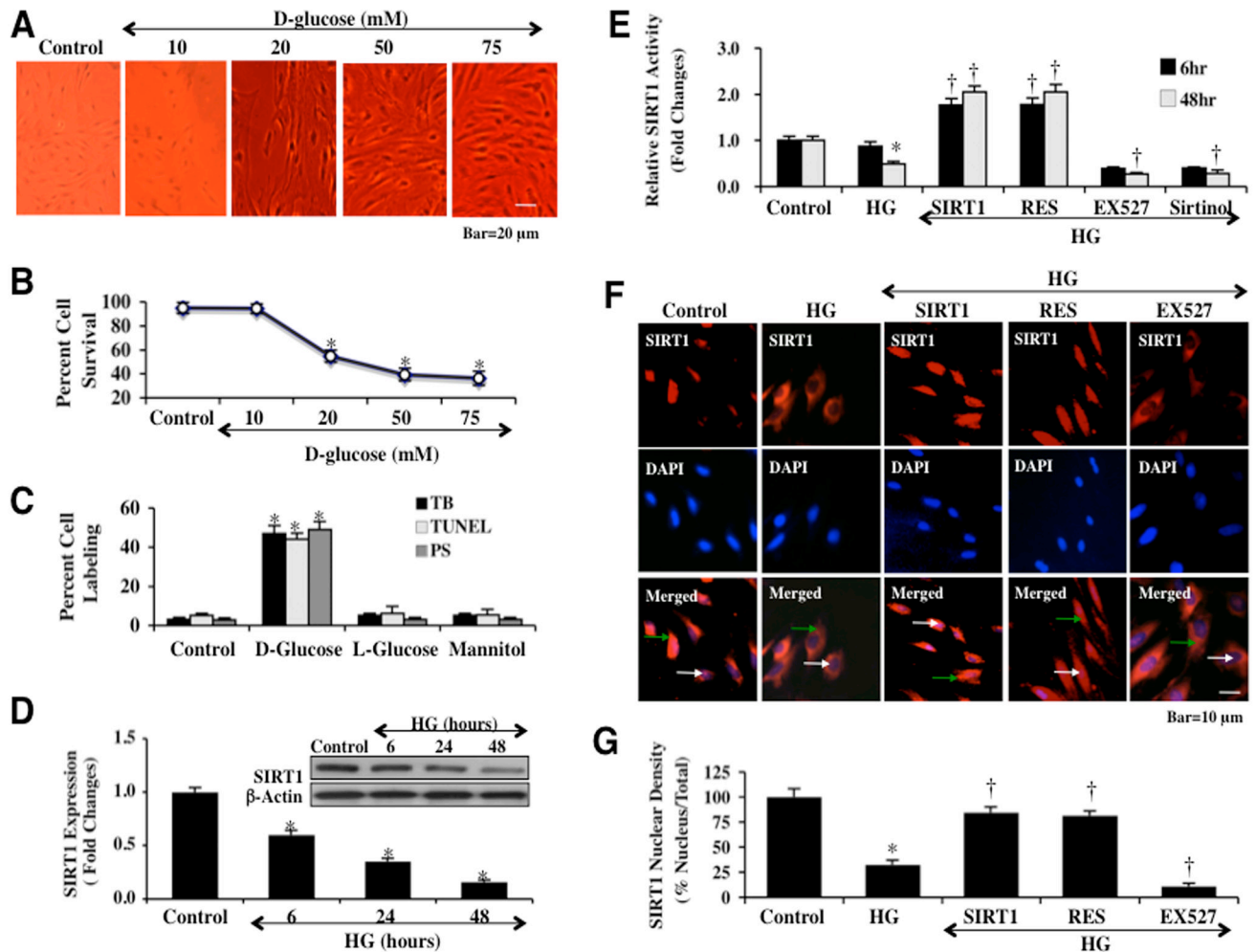


**Fig. (1). Elevated D-glucose exposure injures ECs and prevents endogenous SIRT1 expression, but SIRT1 nuclear translocation is preserved during SIRT1 activation**

(A) Primary cerebral ECs were exposed to elevated D-glucose at the concentrations of 10, 20, 50, 75 mM and EC survival was determined 48 hours later. Representative images illustrate increased trypan blue staining during elevated glucose. (B) Quantification of data demonstrates that EC survival was significantly decreased to  $53 \pm 5\%$  (20 mM),  $41 \pm 5\%$  (50 mM), and  $33 \pm 5\%$  (75 mM) following administration of elevated D-glucose when compared with untreated control cultures ( $98 \pm 3\%$ ,  $*P < 0.01$  vs. Control). Each data point represents the mean and SEM from 6 experiments. (C) Hyperosmolarity or L-glucose do not play a significant role in EC toxicity. D-glucose (20 mM), L-glucose (20 mM), and mannitol (20 mM) were administered to primary cerebral ECs and cell injury with trypan blue (TB), apoptotic phosphatidylserine (PS) exposure, and apoptotic DNA fragmentation (TUNEL) were assessed 48 hours later. Each data point represents the mean and SEM from 6 experiments ( $*P < 0.01$  vs. Control). In D, primary EC protein extracts (50  $\mu$ g/lane) were immunoblotted with anti-SIRT1 (SIRT1) at 6, 24, and 48 hours following administration of elevated D-glucose (HG = high glucose, 20 mM). SIRT1 expression is progressively and significantly reduced at 6, 24 and 48 hours following elevated D-glucose exposure ( $*P < 0.01$  vs. control). In E, activators of SIRT1 with SIRT1 protein (2  $\mu$ M) (SIRT1) and resveratrol (15  $\mu$ M) (RES) and inhibitors of SIRT1 with EX527 (2  $\mu$ M) (EX527) and sirtinol (75  $\mu$ M) (Sirtinol) were assessed with their ability to alter SIRT1

HDAC activity at 6 hours and 48 hours following elevated D-glucose (20 mM) (HG) exposure. SIRT1 protein and resveratrol significantly increased HDAC in ECs while EX527 and sirtinol blocked HDAC activity (\* $P < 0.01$  vs. HG; † $P < 0.01$  vs. untreated ECs = Control). Each data point represents the mean and SEM from 6 experiments. In F and G, ECs were imaged 48 hours following elevated D-glucose (HG = high glucose, 20 mM) with immunofluorescent staining for SIRT1 (Texas-red streptavidin). Nuclei of ECs were counterstained with DAPI. In merged images, untreated control ECs do not have visible nuclei (red in color, white arrows) that illustrate nuclear localization of SIRT1. However, merged images after elevated D-glucose show ECs with distinctly blue nuclei and red cytoplasm (green arrows) illustrating that SIRT1 is confined to the cytoplasm. In addition, inhibition of SIRT1 catalytic activity with EX527 (2  $\mu$ M) during elevated D-glucose exposure also confined SIRT1 to the cytoplasm to a greater degree than during elevated D-glucose alone. Yet, activation of SIRT1 with SIRT1 protein (2  $\mu$ M) or resveratrol (RES) (15  $\mu$ M) during elevated D-glucose maintained SIRT1 in the nucleus of ECs and promoted the trafficking of SIRT1 from the cytoplasm (\* $P < 0.01$  vs. untreated ECs = Control; † $P < 0.01$  vs. HG). Quantification of the intensity of SIRT1 nuclear staining was performed using the public domain NIH Image program (<http://rsb.info.nih.gov/nih-image>). Each data point represents the mean and SEM from 6 experiments.

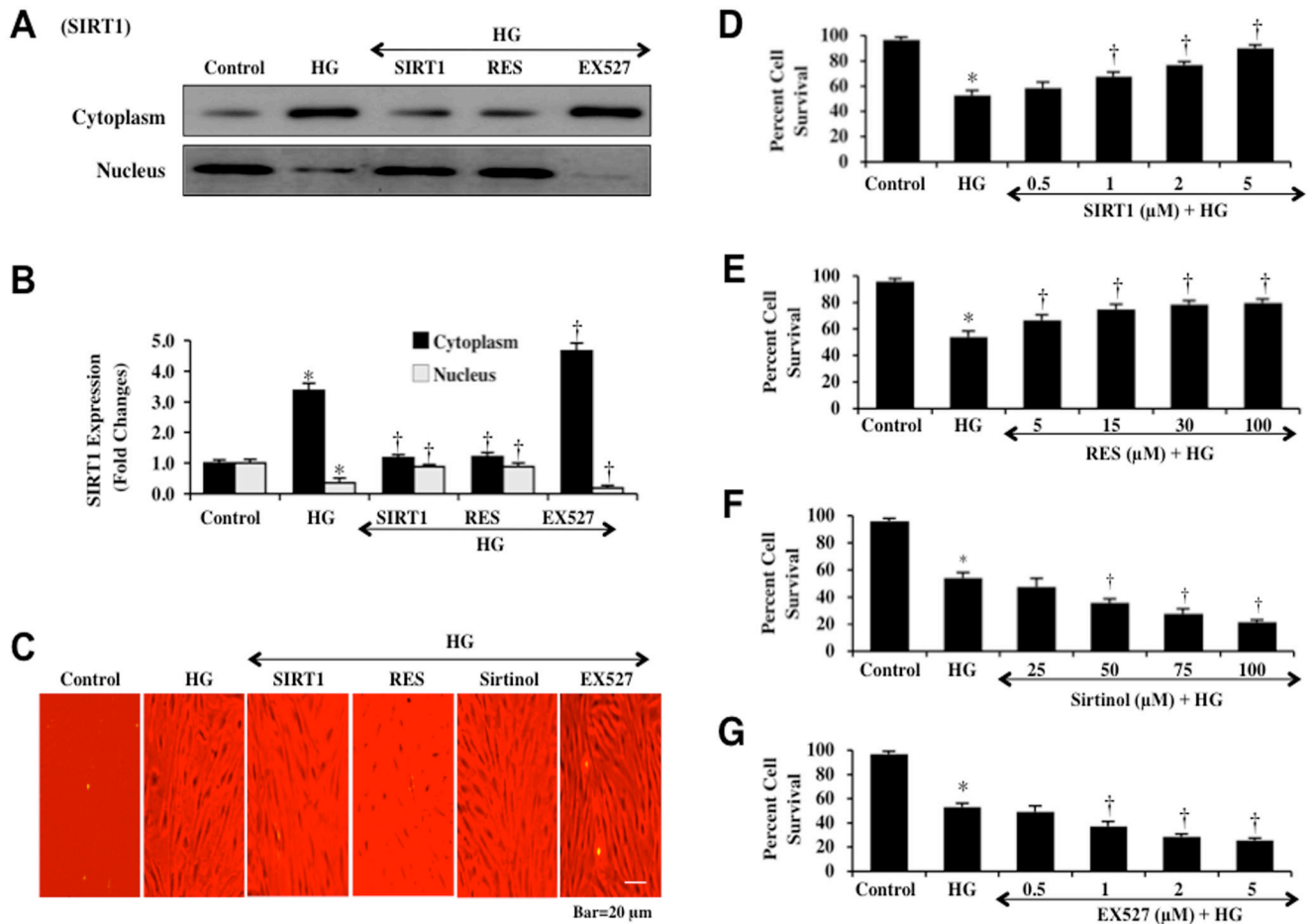


**Fig. (2). Western analysis of SIRT1 translocation and activation of SIRT1 increases EC survival during elevated D-glucose**

In **A** and **B**, equal amounts of cytoplasmic (cytoplasm) or nuclear (nucleus) protein extracts (50  $\mu$ g/lane) were immunoblotted with anti-SIRT1 at 48 hours following administration of elevated D-glucose (HG = high glucose, 20 mM). At 48 hours following elevated D-glucose (20 mM) (HG), SIRT1 is confined to the cytoplasm of ECs, but SIRT1 protein (2  $\mu$ M) (SIRT1) or resveratrol (15  $\mu$ M) (RES) leads to the translocation of endogenous SIRT1 from the cytoplasm to the nucleus. Inhibition of SIRT1 catalytic activity with EX527 (2  $\mu$ M) (EX527) prevents the translocation of SIRT1 to the nucleus to a greater extent than during elevated D-glucose alone. In **C**, primary cerebral ECs were exposed to elevated D-glucose (HG = high glucose, 20 mM) and EC survival was determined 48 hours later. Representative images illustrate increased trypan blue staining during elevated D-glucose and during inhibition of SIRT1 activity with sirtinol (75  $\mu$ M) or EX527 (2  $\mu$ M). Yet, EC survival is increased and trypan blue uptake is reduced during activation of SIRT1 with SIRT1 protein (2  $\mu$ M) or with resveratrol (RES) (15  $\mu$ M) in the presence of elevated D-glucose (20 mM). In **D** and **E**, increasing concentrations of SIRT1 protein or resveratrol (RES) result in significantly increased EC survival during elevated D-glucose (HG = high glucose, 20 mM). In **F** and **G**, inhibition of SIRT1 with increased concentrations of sirtinol or EX527 during elevated D-glucose (HG = high glucose, 20 mM) led to progressive cell injury. In all cases control = untreated ECs (\* $P$ <0.01 vs. untreated ECs = Control; † $P$ <0.01 vs. HG). Each data point represents the mean and SEM from 6 experiments.

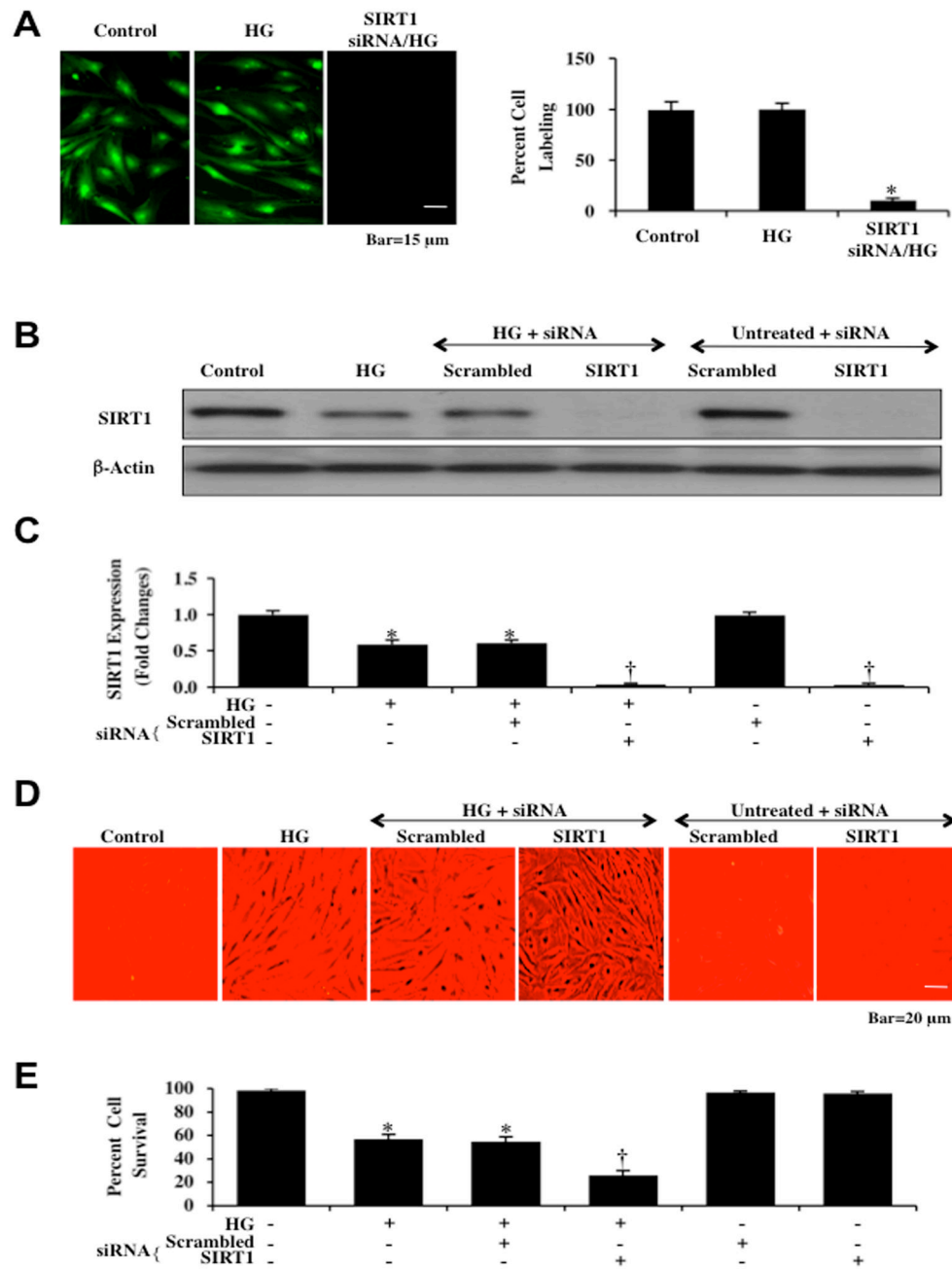


**Fig. (3). Gene knockdown of *SIRT1* worsens EC injury during elevated D-glucose to suggest a role for *SIRT1* endogenous cellular protection**

In **A**, transfection of siRNA against *SIRT1* was performed in ECs and the expression of *SIRT1* protein was assessed by immunofluorescence. In ECs with *SIRT1* gene knockdown, no significant expression of *SIRT1* protein is present ( $*P < 0.01$  vs. untreated ECs = Control or HG). In **B** and **C**, EC protein extracts (50  $\mu$ g/lane) were immunoblotted with anti-*SIRT1* (*SIRT1*) at 6 hours following elevated D-glucose (HG = high glucose, 20 mM). Gene knockdown of *SIRT1* was performed with transfection of *SIRT1* siRNA (siRNA). *SIRT1* siRNA significantly reduced expression of *SIRT1* protein in untreated ECs or following elevated D-glucose (HG = high glucose, 20 mM). Non-specific scrambled siRNA did not

significantly alter SIRT1 expression during elevated D-glucose ( $*P < 0.01$  vs. untreated ECs = Control;  $\dagger P < 0.01$  vs. HG). Quantification of the western band intensity was performed using the public domain NIH Image program (<http://rsb.info.nih.gov/nih-image>). In **D** and **E**, gene knockdown of *SIRT1* with SIRT1 siRNA (siRNA) significantly decreased EC survival to a greater degree than elevated D-glucose alone assessed by trypan blue staining 48 hours after elevated D-glucose exposure (HG = high glucose, 20 mM), suggesting that endogenous level of SIRT1 in ECs is protective against EC injury. SIRT1 siRNA alone and non-specific scrambled siRNA were not toxic. In addition, non-specific scrambled siRNA did not change cell survival when compared to elevated D-glucose alone ( $*P < 0.01$  vs. untreated ECs = Control;  $\dagger P < 0.01$  vs. HG). Each data point represents the mean and SEM from 6 experiments.



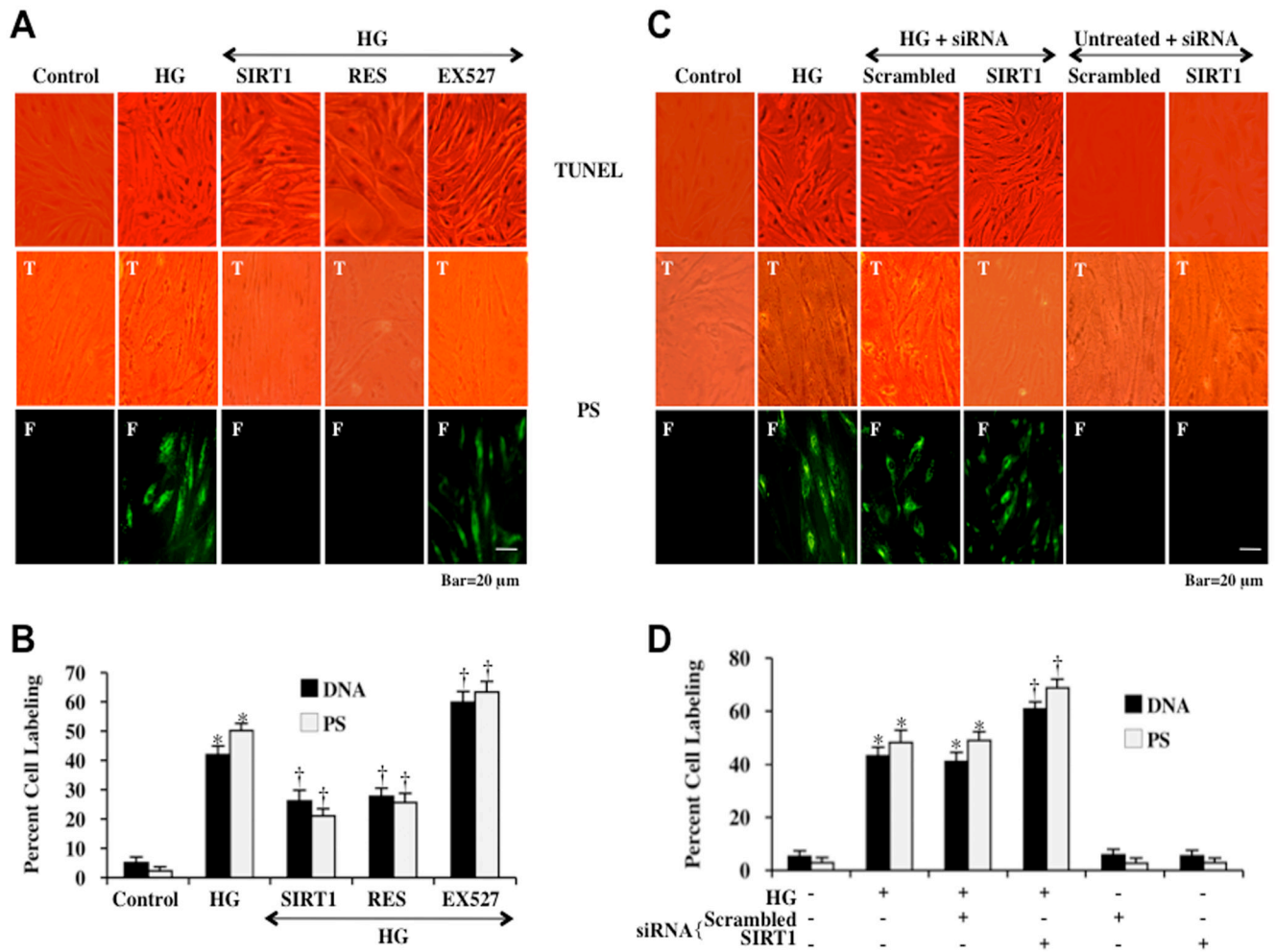


**Fig. (4). Activation of SIRT1 prevents apoptotic early phosphatidylserine (PS) exposure and subsequent nuclear DNA degradation in ECs during elevated D-glucose**  
 In **A** and **B**, representative images illustrate that activation of SIRT1 with SIRT1 protein (2  $\mu$ M) or with resveratrol (RES) (15  $\mu$ M) in the presence of elevated D-glucose (HG = high glucose, 20 mM) significantly blocks EC genomic DNA degradation assessed by TUNEL and membrane PS externalization with transmitted (T) light and corresponding fluorescence (F) assessed by annexin V phycoerythrin (green fluorescence). In contrast, inhibition of SIRT1 activity with EX527 (2  $\mu$ M) (A) or during gene knockdown of *SIRT1* with siRNA (C) lead to greater DNA fragmentation and membrane PS exposure than elevated D-glucose alone, suggesting that an endogenous level of SIRT1 provides protection against apoptotic early and late programs. Non-specific scrambled siRNA did not alter DNA fragmentation or membrane PS exposure in untreated controls or during elevated D-glucose. In **B** and **D**, quantification of data illustrates that DNA fragmentation and membrane PS externalization were significantly increased following elevated D-glucose (HG = high glucose, 20 mM) when compared to untreated EC control cultures, but activation of SIRT1 with SIRT1 protein (2  $\mu$ M) or with resveratrol (RES) (15  $\mu$ M) prevents DNA fragmentation and membrane PS exposure during elevated D-glucose (\* $P$ <0.01 vs. untreated ECs = Control; † $P$ <0.01 vs. HG). Inhibition of SIRT1 with EX527 (2  $\mu$ M) or during gene knockdown of *SIRT1* with siRNA significantly worsens apoptotic injury. SIRT1 siRNA alone was not toxic and non-specific scrambled siRNA

did not alter EC survival during elevated D-glucose. Each data point represents the mean and SEM from 6 experiments.

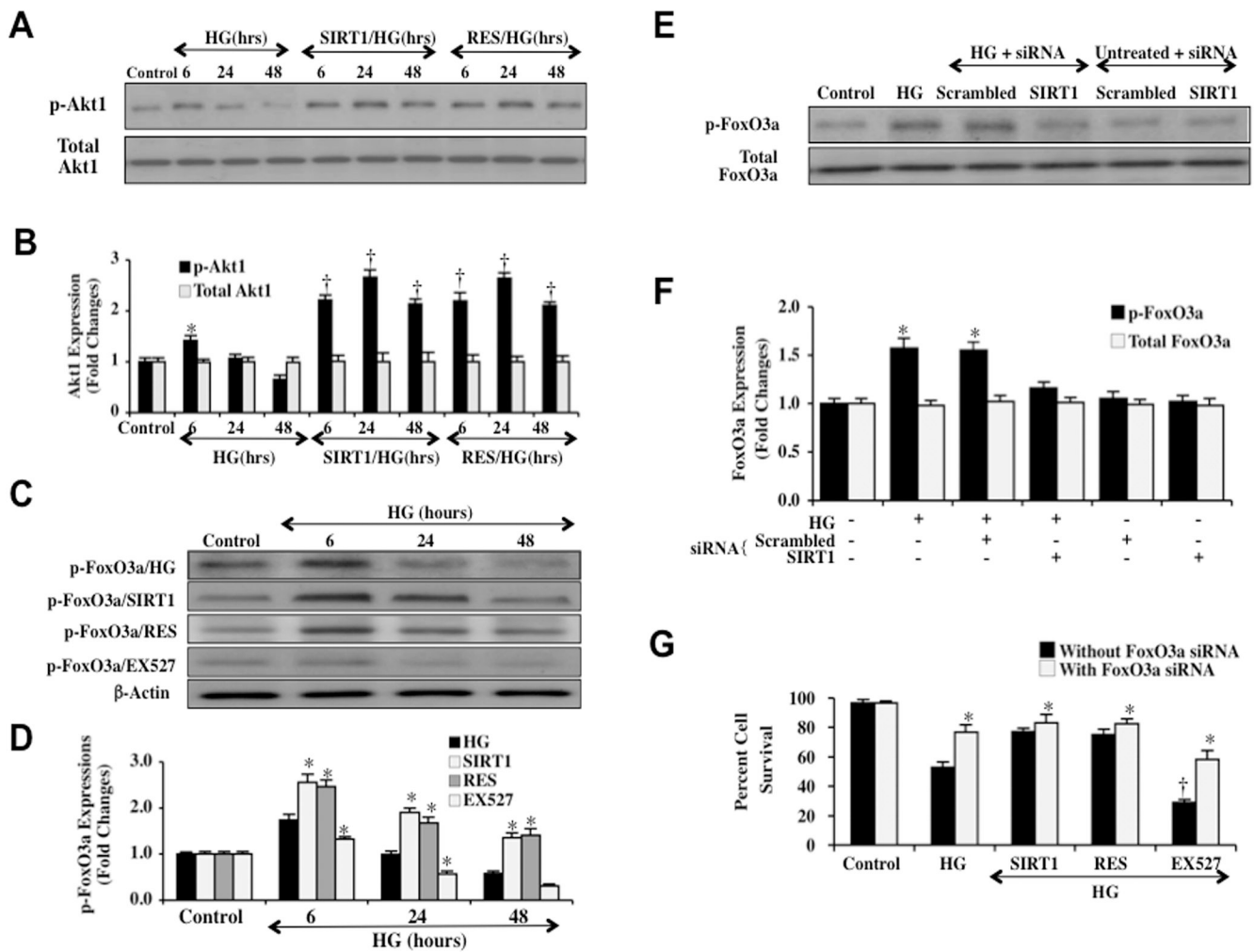


**Fig. (5). SIRT1 activates Akt1 and maintains inhibitory phosphorylation of p-FoxO3a and relies upon p-FoxO3a inhibition for EC protection during elevated D-glucose**

In **A** and **B**, primary EC protein extracts (50  $\mu$ g/lane) were immunoblotted with anti-phosphorylated-Akt1 (p-Akt1, Ser<sup>473</sup>) or anti-total Akt1 at 6, 24, and 48 hours following administration of elevated D-glucose (HG = high glucose, 20 mM). Phosphorylated (active) Akt1 (p-Akt1) expression is initially increased at 6 hours following elevated D-glucose, but subsequently is reduced and returns to control levels at 24 hours and 48 hours after elevated D-glucose (\* $P$ <0.01 vs. control). Total Akt1 is not altered. In **C**, **D**, **E**, and **F**, primary EC protein extracts (50  $\mu$ g/lane) were immunoblotted with anti-phosphorylated-FoxO3a (p-FoxO3a, Ser<sup>253</sup>) or anti-total FoxO3a at 6, 24, and 48 hours following administration of elevated D-glucose (HG = high glucose, 20 mM). Quantification of western band intensity was performed using the public domain NIH Image program (<http://rsb.info.nih.gov/nih-image>). During elevated D-glucose and correlating with Akt1 activity, phosphorylated (inactive) FoxO3a (p-FoxO3a) expression is initially increased at 6 hours but then significantly reduced at 24 hours and at 48 hours (C and D) following elevated D-glucose but total FoxO3a expression (E) is not affected (\* $P$ <0.01 vs. control). Activation of SIRT1 with SIRT1 protein (2  $\mu$ M) or with resveratrol (RES) (15  $\mu$ M) maintained the expression of p-FoxO3a at 6, 24, and 48 hours to a greater degree than during elevated D-glucose (20 mM) exposure alone. In contrast, inhibition of SIRT1 activity with EX527 (2  $\mu$ M) sharply reduced p-FoxO3a expression below

levels for elevated D-glucose alone at 6 and 24 hours and at similar levels to elevated D-glucose alone at 48 hours (A and B). In **E** and **F**, gene knockdown of *SIRT1* with siRNA significantly reduced p-FoxO3a expression at 6 hours below levels observed with elevated D-glucose alone, but expression of total FoxO3a remained unchanged, suggesting that the loss of SIRT1 protein only affected phosphorylation of FoxO3a and that the total FoxO3a protein was not degraded. In **G**, transfection with FoxO3a siRNA increased EC survival during elevated D-glucose (HG = high glucose, 20 mM) alone and also produced equal protective capacity and increased survival in ECs assessed by trypan blue uptake during either SIRT1 protein (2  $\mu$ M) or resveratrol (RES) (15  $\mu$ M) application at 48 hours after elevated D-glucose. Gene knockdown of *FoxO3a* also reversed EC injury during SIRT1 inhibition with EX527 (2  $\mu$ M) (\* $P$ <0.01 vs. HG without FoxO3a siRNA; † $P$ <0.01 vs. HG without FoxO3a siRNA). Control = untreated cells and each data point represents the mean and SEM from 6 experiments.

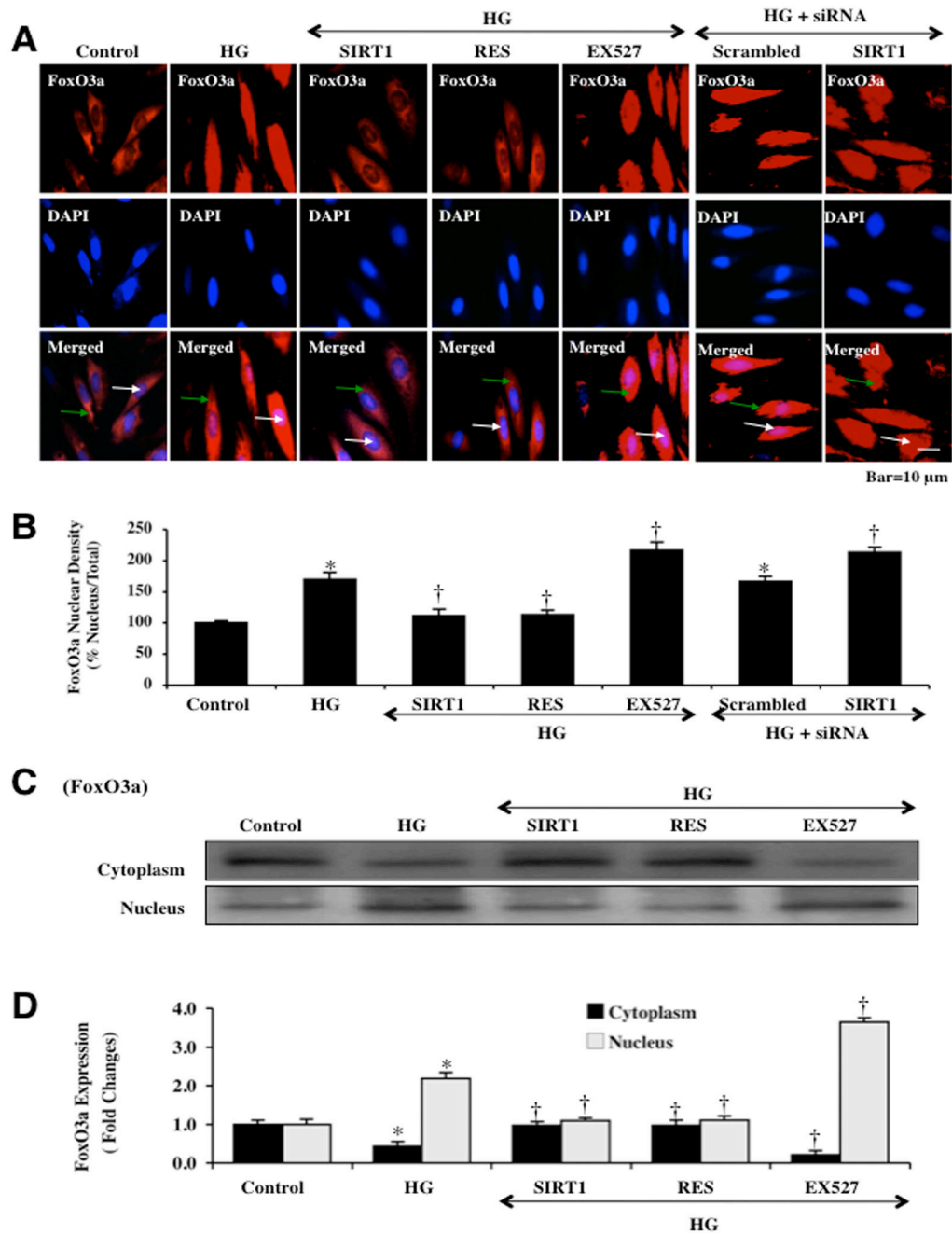


**Fig. (6). SIRT1 activation blocks nuclear translocation of FoxO3a in ECs during elevated glucose**  
 In **A** and **B**, ECs were imaged 48 hours following elevated D-glucose (HG = high glucose, 20 mM) with immunofluorescent staining for FoxO3a (Texas-red streptavidin). Nuclei of ECs were counterstained with DAPI. In merged images, untreated control ECs have visible nuclei (dark blue in color, white arrows) that illustrate absence of FoxO3a in the nucleus. Merged images after elevated D-glucose demonstrate ECs with completely red cytoplasm (green arrows) and no visible nucleus with DAPI illustrating translocation of FoxO3a to the nucleus. Activation of SIRT1 with SIRT1 protein (2 μM) or resveratrol (RES) (15 μM) during elevated D-glucose maintains FoxO3a in the cytoplasm of ECs (\**P*<0.01 vs. untreated ECs = Control; †*P*<0.01 vs. HG). However, inhibition of SIRT1 catalytic activity with EX527 (2 μM) or gene



knockdown of *SIRT1* with transfection of *SIRT1* siRNA (siRNA) during elevated D-glucose allows FoxO3a to translocate to the nucleus (\* $P < 0.01$  vs. untreated ECs = Control; † $P < 0.01$  vs. HG). Non-specific scrambled siRNA did not alter total FoxO3a translocation during elevated D-glucose. Quantification of the intensity of FoxO3a nuclear staining was performed using the public domain NIH Image program (<http://rsb.info.nih.gov/nih-image>). Each data point represents the mean and SEM from 6 experiments. In **C** and **D**, equal amounts of cytoplasmic (cytoplasm) or nuclear (nucleus) protein extracts (50  $\mu$ g/lane) were immunoblotted with anti-FoxO3a at 48 hours following administration of elevated D-glucose (HG = high glucose, 20 mM). At 48 hours following elevated D-glucose (20 mM) (HG) alone or with inhibition of *SIRT1* activity with EX527 (2  $\mu$ M) (EX527), FoxO3a translocates from the cytoplasm to the nucleus. In contrast, activation of *SIRT1* with *SIRT1* protein (2  $\mu$ M) (*SIRT1*) or resveratrol (15  $\mu$ M) (RES) blocks subcellular translocation of FoxO3a from the cytoplasm to the cell nucleus.

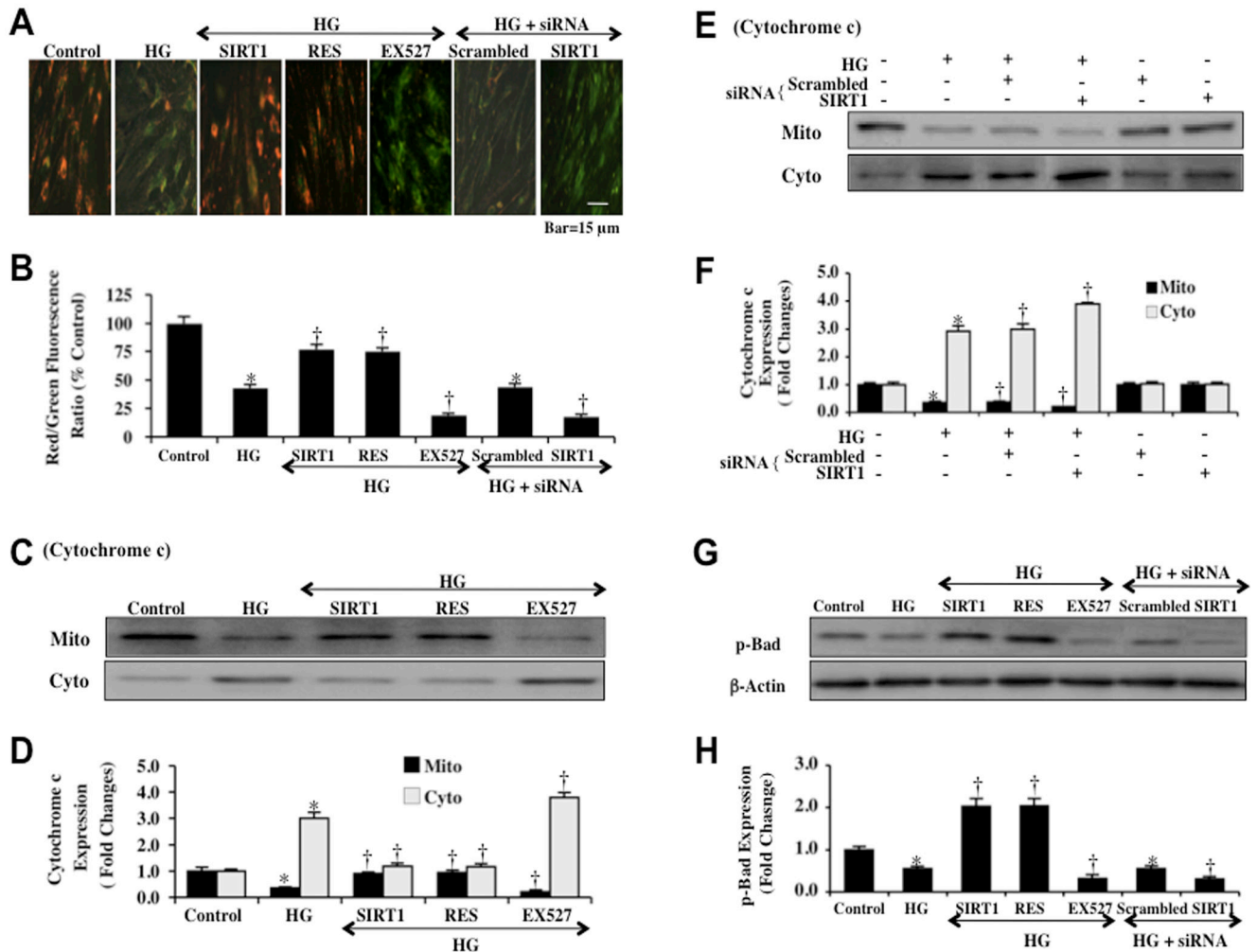


**Fig. (7). SIRT1 inhibits mitochondrial depolarization, prevents the release of cytochrome c, and maintains activation of Bad**

In **A**, elevated D-glucose (HG = high glucose, 20 mM) leads to a significant decrease in the red/green fluorescence intensity ratio of mitochondria using the cationic membrane potential indicator JC-1 within 24 hours when compared with untreated control ECs, demonstrating that elevated D-glucose leads to mitochondrial membrane depolarization. Activation of SIRT1 with SIRT1 protein (2 μM) or resveratrol (RES) (15 μM) during elevated D-glucose significantly increased the red/green fluorescence intensity of mitochondria in ECs, demonstrating that mitochondrial membrane potential was restored. In contrast, inhibition of SIRT1 activity with EX527 (2 μM) and gene knockdown of *SIRT1* with transfection of SIRT1 siRNA (siRNA) worsened mitochondrial membrane depolarization to a greater degree than during elevated D-glucose exposure alone. Transfection with non-specific scrambled siRNA also did not prevent mitochondrial membrane depolarization during elevated D-glucose exposure. In **B**, the relative ratio of red/green fluorescent intensity of mitochondrial staining in untreated control ECs, in ECs exposed to elevated D-glucose (HG = high glucose, 20 mM), during SIRT1 activation, or during SIRT1 inactivation was measured in 6 independent experiments with analysis performed using the public domain NIH Image program (<http://rsb.info.nih.gov/nih-image>) (untreated ECs = Control vs. HG, \* $P < 0.01$ ; SIRT1 activity vs. HG, † $P < 0.01$ ). In **C** and **E**, equal amounts of mitochondrial (mito) or cytosol (cyto) protein extracts (50 μg/lane) were

immunoblotted demonstrating that SIRT1 activation (SIRT1 protein, RES) significantly prevented cytochrome c release from mitochondria 24 hours after elevated D-glucose (HG = high glucose, 20 mM). SIRT1 inhibition (EX527, SIRT1 siRNA) and non-specific scrambled siRNA did not prevent cytochrome c release during elevated D-glucose. In D and F, quantification of the western band intensity was performed using the public domain NIH Image program (<http://rsb.info.nih.gov/nih-image>) and demonstrates that significant release of cytochrome c occurs 24 hours following elevated D-glucose (HG = high glucose, 20 mM), but activation of SIRT1 with SIRT1 protein (2  $\mu$ M) or resveratrol (RES) (15  $\mu$ M) prevents cytochrome c release from EC mitochondria. Inhibition of SIRT1 activity with EX527 (2  $\mu$ M) (C and D) and gene knockdown of *SIRT1* (E and F) potentiated increased release of cytochrome c. Non-specific scrambled siRNA was ineffective during elevated D-glucose to prevent cytochrome c release and both non-specific siRNA and SIRT1 siRNA alone did not alter mitochondrial cytochrome c in untreated control cells (E and F) (untreated ECs = Control vs. HG, \* $P$ <0.01; SIRT1 activity vs. HG, † $P$ <0.01). Each data point represents the mean and SEM from 6 experiments. In G and H, primary EC protein extracts (50  $\mu$ /lane) were immunoblotted with anti-phosphorylated-Bad (p-Bad, Ser<sup>136</sup>) at 24 hours following administration of elevated D-glucose (HG = high glucose, 20 mM). Phosphorylated (active) Bad (p-Bad) expression is promoted by SIRT1 activation, but is lost during inhibition of SIRT1 or SIRT1 gene knockdown. Non-specific scrambled siRNA during elevated D-glucose did not change Bad phosphorylation as was similar to Bad phosphorylation during elevated D-glucose alone (untreated ECs = Control vs. HG, \* $P$ <0.01; Bad phosphorylation vs. HG, † $P$ <0.01).

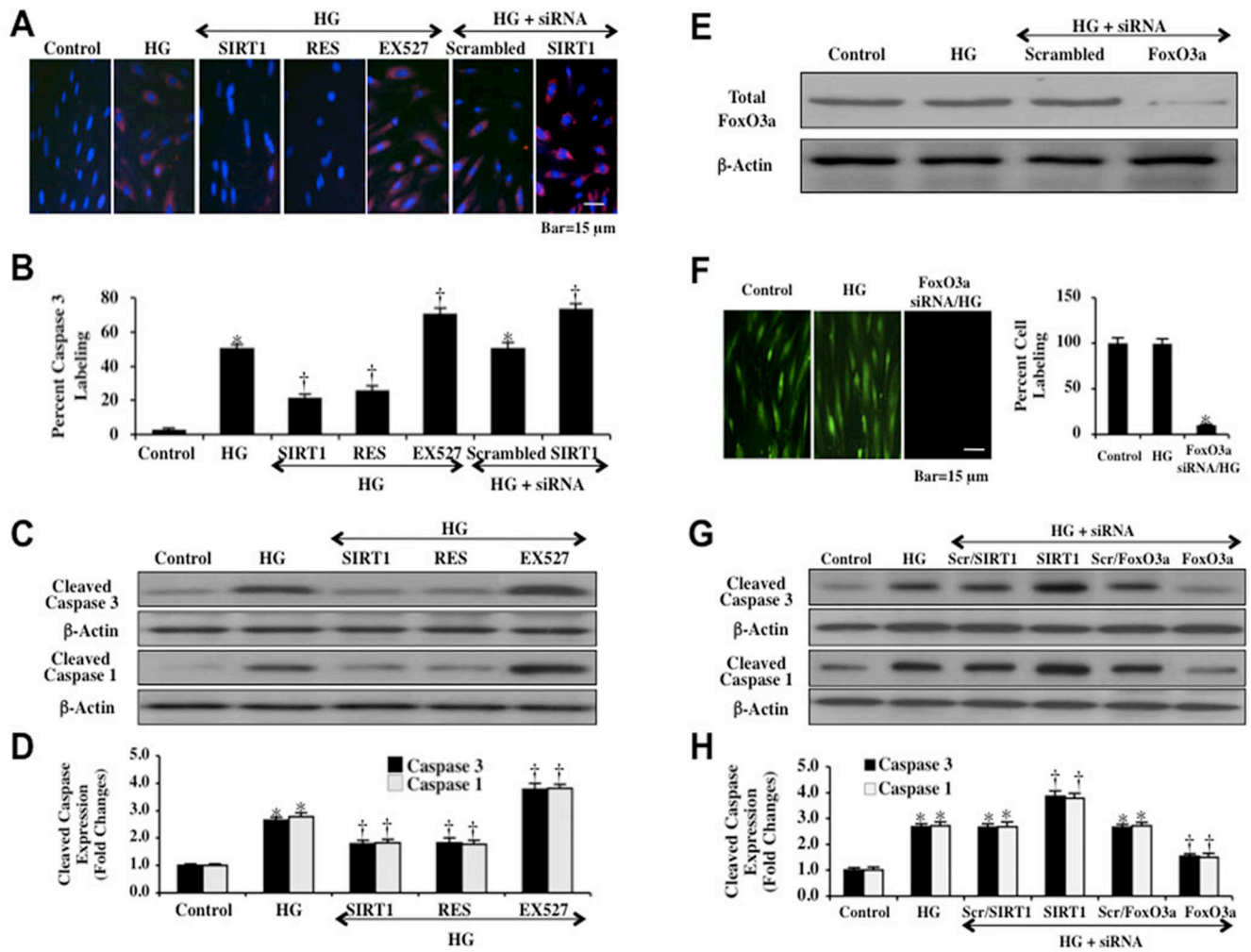


**Fig. (8). SIRT1 controls caspase 1 and caspase 3 activity during elevated D-glucose that employs FoxO3a**

In **A**, ECs were exposed to elevated D-glucose (HG = high glucose, 20 mM) and caspase 3 activation was determined 24 hours after elevated D-glucose exposure through immunocytochemistry with antibodies against cleaved active caspase 3 (17 kDa). Representative images illustrate active caspase 3 staining (red) in cells following elevated D-glucose, but cellular red staining is almost absent during activation of SIRT1 with SIRT1 protein (2 μM) or resveratrol (RES) (15 μM). Inhibition of SIRT1 activity with EX527 (2 μM) or during gene knockdown of *SIRT1* significantly increased active caspase 3 expression to a greater degree in ECs that during elevated D-glucose alone, illustrating that SIRT1 activation was a robust modulator of caspase 3 activity. Non-specific scrambled siRNA did not eliminate caspase 3 activity during elevated D-glucose and both non-specific scrambled siRNA and transfection of SIRT1 siRNA alone did not alter caspase 3 activity in untreated control cells. In **B**, quantification of caspase 3 immunocytochemistry was performed using the public domain NIH Image program (<http://rsb.info.nih.gov/nih-image>) and demonstrates that elevated D-glucose (HG = high glucose, 20 mM) significantly increased the expression of cleaved (active) caspase 3 when compared to untreated control cells. Expression of cleaved (active) caspase 3 was significantly limited during SIRT1 activation (SIRT1 protein, RES), but potentiated to a greater degree with SIRT1 inhibition (EX527, SIRT1 siRNA) than during D-glucose exposure alone (\* $P < 0.01$  vs. untreated ECs = Control; † $P < 0.01$  vs. HG). In **C** and **G**, EC protein extracts

(50  $\mu\text{g}/\text{lane}$ ) were immunoblotted with anti-cleaved caspase 3 product (active caspase 3, 17 kDa) and with anti-cleaved caspase 1 product (active caspase 1, 20 kDa) at 12 hours following elevated D-glucose (HG = high glucose, 20 mM). Elevated D-glucose markedly increased cleaved caspase 3 and caspase 1 expression, but gene knockdown of *FoxO3a* with FoxO3a siRNA (siRNA) significantly blocked cleaved caspase 3 and caspase 1 expression 24 hours after elevated D-glucose. Non-specific scrambled siRNA did not eliminate caspase 3 or caspase 1 activities during elevated D-glucose and both non-specific scrambled siRNA and transfection of FoxO3a siRNA alone did not alter caspase 3 or caspase 1 activities in untreated control cells. In **D** and **H**, quantification of western band intensity was performed using the public domain NIH Image program (<http://rsb.info.nih.gov/nih-image>) and demonstrates that SIRT1 activation (SIRT1 protein, RES) prevents cleaved caspase 3 and caspase 1 expression 24 hours after elevated D-glucose exposure, but SIRT1 inhibition (EX527, SIRT1 siRNA) significantly increases cleaved caspase 3 and caspase 1 expression to a greater degree than with elevated D-glucose alone. Non-specific scrambled siRNA did not reduce cleaved caspase 3 or caspase 1 expression during elevated D-glucose (\* $P < 0.01$  vs. untreated ECs = Control; † $P < 0.01$  vs. HG). SIRT1 siRNA alone in untreated control cells was not toxic. Each data point represents the mean and SEM from 6 experiments. In **E**, EC protein extracts (50  $\mu\text{g}/\text{lane}$ ) were immunoblotted with anti-total FoxO3a (FoxO3a) at 24 hours following elevated D-glucose (HG = high glucose, 20 mM). Gene knockdown of *FoxO3a* was performed with transfection of FoxO3a siRNA (siRNA). FoxO3a siRNA significantly reduced expression of FoxO3a protein in ECs following elevated D-glucose (HG = high glucose, 20 mM). Non-specific scrambled siRNA did not significantly alter total FoxO3a expression during elevated D-glucose. In **F**, transfection of siRNA against FoxO3a was performed in ECs and the expression of total FoxO3a protein was assessed by immunofluorescence. In ECs with FoxO3a gene knockdown, no significant expression of FoxO3a protein is present (\* $P < 0.01$  vs. untreated ECs = Control or HG). In **G** and **H**, gene knockdown of *FoxO3a* with FoxO3a siRNA (siRNA) significantly blocks cleaved (active) caspase 3 and caspase 1 activities 24 hours after elevated D-glucose exposure (HG = high glucose, 20 mM). FoxO3a siRNA alone and non-specific scrambled siRNA were not toxic. In addition, nonspecific scrambled siRNA did not change caspase 1 and caspase 3 activities when compared to elevated D-glucose alone (\* $P < 0.01$  vs. untreated ECs = Control; † $P < 0.01$  vs. HG). Each data point represents the mean and SEM from 6 experiments.